Mechanics of Materials 105 (2017) 16–28

Contents lists available at ScienceDirect

Mechanics of Materials

journal homepage: www.elsevier.com/locate/mechmat

Nonlinear effective properties of heterogeneous materials with ellipsoidal microstructure

Stefano Giordano[a,b,*]

[a] Institute of Electronics, Microelectronics and Nanotechnology (IEMN UMR CNRS 8520), 59652 Villeneuve d'Ascq, France
[b] Joint International Laboratory LIA LEMAC/LICS, École Centrale de Lille, ComUE Lille Nord de France, 59652 Villeneuve d'Ascq, France

ARTICLE INFO

Article history:
Received 5 July 2016
Revised 21 October 2016
Available online 23 November 2016

Keywords:
Heterogeneous material
Nonlinear homogenization
Ellipsoidal microstructure
Ponte Castañeda–Willis estimate

ABSTRACT

The analysis and the synthesis of the nonlinear effective response of particulate composite materials are of great importance for developing new systems such as nonlinear elastic and electromagnetic metamaterials, nonlinear waveguides, nonlinear magnetoelectric devices and photonic or phononic crystals. Typically, classical homogenization schemes take into account the shape of the inhomogenieties but neglect the spatial correlation among them, a crucial feature for the above applications. In this paper we develop a nonlinear homogenization technique for dispersions of nonlinear particles in a linear matrix, which is able to take account of spatial correlation by means of the so-called ellipsoidal microstructure. While the linear result corresponds to the well known Ponte Castañeda–Willis estimate, we propose new formulae for the second and third order nonlinear behavior. We finally show applications to the nonlinear elastic Landau coefficients and to the nonlinear hypersusceptibility of transport processes.

1. Introduction

In recent times, a great number of investigations have been devoted to the elastic and electromagnetic nonlinear properties of particulate composite materials in view of their applications to modern nanotechnology. In fact, the physical nonlinearity of some elements composing a structured system allows for generating a tunable complex behavior, which may exploited to implement specific functions not existing in simple materials. For instance, efficient acoustic diodes have been designed by means of highly nonlinear elastic materials combined with one-dimensional phononic crystals (Liang et al., 2009, 2010) and they can be profitably exploited for thermal management at a microscopic scale (Li et al., 2012). The practical realization of these devices needs elastic materials with precisely tuned strong nonlinearities that can be obtained either through bubbly liquids with optimized concentration of gas (Liang et al., 2010) or soft materials (polymers) with pores (Brunet et al., 2013). Another emerging field is represented by the nonlinear acoustic metamaterials, which are able to control several features of propagating elastic waves (Herbold and Nesterenko, 2013; Manktelow et al., 2011; Kim et al., 2015). The elastic behavior can be coupled with the magnetic one, thus generating magnetoelastic metamaterials, where a new type of nonlinear response arises from this interaction (Lapine et al., 2012). One more example of nonlinear media is given by the granular crystals, which are capable of generating shock-absorbing materials, sound-focusing devices, acoustic switches, and other exotic devices (Porter et al., 2015; Lydon et al., 2015). Similar effects were studied in electrodynamics and optical diodes, transistors and other devices have been realized through non-linear electromagnetic components based on photonic crystals (Mingaleev and Kivshar, 2002; Soljacic and Joannopoulos, 2010). Also, the development of nonlinear electromagnetic metamaterials and plasmonic devices allowed to tune electromagnetic properties with the possibility of controlling the effect of specific nonlinearities (Mary et al., 2008; Kozyrev and van der, 2008; Xu et al., 2009; Lapine et al., 2014). Other largely investigated structures include nonlinear photonic crystals (Berger, 1998), nonlinear optical waveguides (Tsang and Liu, 2008) and nonlinear magnetoelectric devices Rose et al. (2012).

All these applications prove the need of designing heterogeneous materials with controlled elastic and electromagnetic nonlinearities. To do this, we require efficient models to predict the nonlinear behavior of composites as a function of their morphology. This task is usually performed by linear and nonlinear homogenization methods, which determine the effective physical properties of a given microstructure (Nemat-Nasser and Hori, 1993; Milton, 2002; Torquato, 2002; Kanaun and Levin, 2008). Most of the homogenization techniques consider parallel or random orientation of the inhomogeneities, without taking into

* Correspondence address: Institute of Electronics, Microelectronics and Nanotechnology (IEMN UMR CNRS 8520), 59652 Villeneuve d'Ascq, France.
E-mail addresses: Stefano.Giordano@iemn.univ-lille1.fr, stefano.giordano@iemn.univ-lille1.fr

http://dx.doi.org/10.1016/j.mechmat.2016.11.003
0167-6636/

account their real spatial distribution. They have been developed for dealing with, e.g., ellipsoidal particles (Kachanov and Sevostianov, 2005; Giordano, 2003, 2005), cracks (Kachanov, 1994; Giordano and Colombo, 2007b, 2007a), and poroelastic materials (Berryman, 1997; Dormieux et al., 2002). The classical linear theory used for considering the spatial distribution of particles (i.e. their spatial correlation) is based on the Ponte Castañeda–Willis estimate, which takes into account the so-called ellipsoidal microstructure (Ponte Castañeda and Willis, 1995). This result has been derived by considering the Hashin-Shtrikman variational approach in the form developed by Willis (1977, 1978). While in its original form the inclusion shape and spatial distribution are considered jointly (Willis, 1977), in the second version these two features are introduced separately (Willis, 1978). This point is crucial to derive the Ponte Castañeda–Willis estimate, which considers arbitrary ellipsoidal particles and, independently, assumes the hypothesis of ellipsoidal symmetry for the spatial distribution of the particles. The result represents a generalization of the classical Mori and Tanaka's (1973) scheme, always giving tensors of effective moduli satisfying the necessary symmetry requirements (Ponte Castañeda and Willis, 1995). The relation between the Ponte Castañeda–Willis and Mori–Tanaka schemes has been thoroughly examined in the literature (Hu and Weng, 2000b, 2000a; Weng, 2010). From the point of view of the applications, the Ponte Castañeda–Willis estimate has been used to investigate the mechanical properties of multifractured materials (Dormieux and Kondo, 2016), nanocomposites (Cauvin et al., 2010), rocks (Wendt et al., 2003; Gruescu et al., 2007), and the response of magnetostrictive (Galipeau and Ponte Castañeda, 2012) or magneto-electro-elastic composites (Franciosi, 2013). It is important to remark that the variational principles have been also used for nonlinear composites with both nonlinear comparison solid (Talbot and Willis, 1985, 1987) and linear comparison solid (Ponte Castañeda, 1991, 1992; Suquet, 1993; Ponte Castañeda and Suquet, 1998).

In this paper, we approach the problem of determining the nonlinear effective properties of a composite materials described by the so-called ellipsoidal microstructure or, equivalently, by the ellipsoidal symmetry for the spatial distribution of particles. It means that the microstructure can be described by a population of arbitrary ellipsoidal particles exhibiting a specific nonlinearity, embedded in a linear matrix with a spatial distribution given by an arbitrary ellipsoidal correlation. By introducing a two-step multiscale procedure we can obtain the linear and nonlinear (second order and third order) physical properties of the heterogeneous material. We take into account ellipsoidal inhomogeneities of arbitrary shape and an arbitrary ellipsoidal correlation among particles. This allows to write the final linear and nonlinear effective properties in terms of two independent Eshelby tensors describing shape and distribution, respectively. The linear result coincides with the Ponte Castañeda–Willis estimate whereas the closed form expression for the nonlinear effective tensor represents a new achievement, which is explicit and well suited for the applications. We remark that all results can be also used in dynamic regime if we consider the wavelength of the propagating wave much larger than the particles size. In this case we are working in the so-called quasi-static regime and any inhomogeneity feels a nearly static applied field. Interestingly enough, although we show explicit examples analysing elastic and transport properties, the proposed scheme can be easily adopted to homogenize the fully coupled thermo-magneto-electro-elastic case as well.

The proposed methodology can be adopted for modeling novel composites behaviors but also for validating advanced numerical models and multiscale techniques largely used for the description of materials with random microstructure. Usually, these methodologies are based on boundary value problems defined on finite-size mesoscales (Ghosh, 2011; Salmi et al., 2012), sometimes generalized to consider non-classical materials such as, e.g., micropolar continua (Trovalusci et al., 2014, 2015). The central issue of these approaches, applied to random microstructures, concerns the proper definition of Representative Volume Element (RVE) (Ostoja-Starzewski, 2006). Since the proposed model, being entirely theoretical, does not require the RVE estimation, the comparison with numerical approaches can be useful to further validate the RVE selection process.

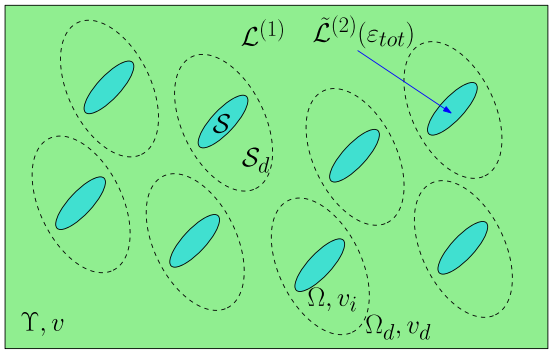

Fig. 1. Distribution of particles embedded in the matrix $\mathcal{L}^{(1)}$ showing the so-called ellipsoidal microstructure. Each nonlinear inhomogeneity (region Ω) has a volume $v_i = \text{mes}(\Omega)$, an Eshelby tensor $\mathcal{S}$ and a stiffness tensor $\tilde{\mathcal{L}}^{(2)}(\varepsilon_{tot})$. Moreover, all particles are surrounded by a security ellipsoidal surface Ω_d, having volume v_d and Eshelby tensor $\mathcal{S}_d$.

The structure of the paper follows. In Section 2, we introduce the problem statement, by defining the ellipsoidal microstructure and the related nonlinear homogenization issues. In Section 3, we review the Eshelby formalism for both linear and nonlinear inhomogeneities. In Section 4, we approach the first step of the multiscale procedure: we solve the homogenization problem for a nonlinear composite ellipsoid. In Section 5, we elaborate the second step of the homogenization: we determine the effective behavior of the dispersion of nonlinear inhomogeneities. In Section 6, we combine the two procedure in order to get the final results. Finally, in Sections 7 and 8 we show some applications to the second order nonlinear elastic Landau coefficients and to the third order nonlinear hypersusceptibility of transport processes.

2. Problem statement

We define here the microstructure and the methodology adopted in this work. The geometry of the system is represented in Fig. 1, where a population of inhomogeneities are dispersed in a linear matrix of stiffness $\mathcal{L}^{(1)}$. Each nonlinear inhomogeneity is characterized by an ellipsoidal region Ω, a volume $v_i = \text{mes}(\Omega)$, and an Eshelby tensor $\mathcal{S}$. Its nonlinear elastic response is characterized by a strain-dependent stiffness tensor $\tilde{\mathcal{L}}^{(2)}(\varepsilon_{tot})$. Moreover, every particle is surrounded by another ellipsoidal surface Ω_d, having internal volume v_d and Eshelby tensor $\mathcal{S}_d$. This is the so-called security surface and allows us to define the ellipsoidal symmetry for the spatial distribution of particles: the security regions of any couple of inhomogeneities cannot be overlapped. This principle imposes the spatial correlation among particles and may generate a form of anisotropy induced by the distribution of particles position. Indeed, even if we consider spherical inhomogenities, the overall behavior of the heterogeneous material will be anisotropic if the security surface are ellipsoidal.

It is important to remark that the (centres of the) inhomogeneities are uniformly randomly distributed within the material volume, provided that they are not overlapping (the composite is statistically homogeneous). It means that the probability density for finding an inclusion at a given position is a constant. However,

the joint probability density for finding a first inhomogeneity centered at a point $\vec{x}$ and second inhomogeneity centered at another point $\vec{x}'$ is a scalar function of $\vec{x}-\vec{x}'$. This function is defined by the security surfaces, which impose the hypothesis of ellipsoidal symmetry for the distribution of inhomogeneities (Ponte Castañeda and Willis, 1995). This corresponds to the statistical anisotropy of the microstructure. The statistical isotropy can be simply obtained by considering the particular case of spherical security surfaces. We also underline that the security surfaces must be considered parallel in order to effectively induce the ellipsoidal symmetry, i.e., the statistical anisotropy. However, the inhomogeneities within the security surfaces may be considered either aligned or randomly oriented. While in the present paper we consider aligned inhomogeneities, we postpone the analysis of the random orientations to a future investigation.

The original point of this work is that we take account of the particles nonlinearity, whereas the classical Ponte Castañeda–Willis estimate considers linear inhomogeneities. To approach the problem, we firstly exactly solve the homogenization issue within the surface Ω_d (nonlinear composite ellipsoid) and then we determine the effective properties of the dispersion of homogenized ellipsoids through a generalized (nonlinear) Mori–Tanaka scheme. We emphasize the effectiveness of the double step multiscale approach taking account the constitutive nonlinearity at the underling level and the statistical distribution at the intermediate level, as many computational methods propose.

We also remark that we considered nonlinear particles embedded in a linear matrix since the possible matrix nonlinearity makes the Eshelby theory not applicable to determine the internal elastic fields. Indeed, strain and stress fields within a nonlinear particle embedded in a nonlinear matrix are in general not uniform and must be determined with *ad hoc* methodologies (Palla et al., 2010) leading to specific homogenization theories (Giordano, 2013). However, we underline that the nonlinearity is typically confined within the embedded particles in most of technological applications.

To conclude the problem definition, we finally observe that in our homogenization scheme we did not consider the nonlocal character of the macroscopic constitutive equation, typically emerging in higher order homogenization. Indeed, if we consider a heterogeneous RVE with boundary conditions fixing the displacement field through linear and quadratic terms, we obtain an effective energy density which is quadratic in the strain tensor and quadratic in the derivatives of the strain tensor. Hence, this energy form defines second-gradient elastic materials (Bacca et al., 2013a; Bacca et al., 2013b). Here, we neglect this aspect, i.e., we implicitly study only the first energy term, quadratic in the strain tensor.

3. Eshelby formalism: linear and nonlinear inhomogeneity

To begin, we take into consideration a linear and homogeneous elastic matrix described by the constitutive equation $T=\mathcal{L}^{(1)}\varepsilon$ (T is the stress tensor, ε the strain tensor, and $\mathcal{L}^{(1)}$ the stiffness tensor), where an inclusion is embedded within the region Ω (see Fig. 2). The latter is described by the constitutive equation $T=\mathcal{L}^{(1)}(\varepsilon-\varepsilon^*)$, where ε^* represents an eigenstrain uniformly distributed in Ω (Li and Wang, 2008; Mura, 1987; Qu and Cherkaoui, 2006). As widely described in literature, the solution of the inclusion problem is given by

$$\varepsilon_{nm}=\mathcal{S}_{nmhk}\varepsilon^*_{hk}, \tag{1}$$

at any point of the space (Mura, 1987; Qu and Cherkaoui, 2006; Li and Wang, 2008). Here, we introduced the Eshelby tensor, whose

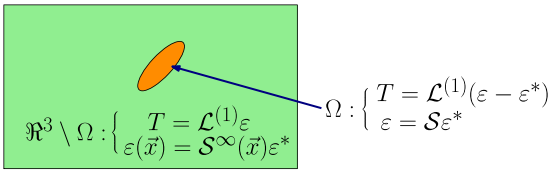

Fig. 2. Scheme of an inclusion characterized by an eigenstrain ε^* and elastic fields within and outside Ω.

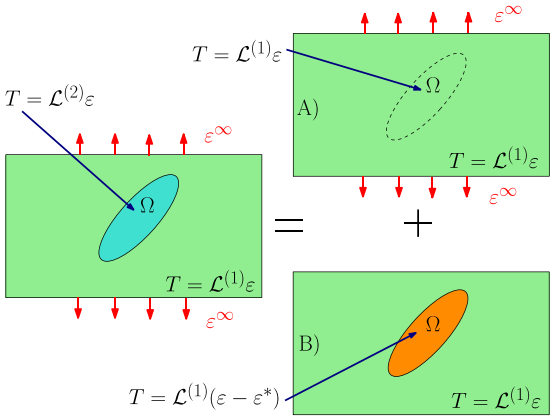

Fig. 3. Scheme of the equivalence principle used to solve the inhomogeneity problem. The inhomogeneity is equivalent to the superposition of the configurations A) (homogeneous medium loaded by ε^{∞}) and B) (uniform inclusion with eigenstrain ε^*).

general expression follows (Eshelby, 1957, 1959)

$$\mathcal{S}_{nmhk}(\vec{x})=-\mathcal{L}^{(1)}_{ijhk}\int_{\Omega\subset\Re^3}\Gamma_{nmij}(\vec{x}-\vec{x}')d\vec{x}', \tag{2}$$

where Γ is the modified Green tensor (Kröner, 1990)

$$\Gamma_{nmij}(\vec{z})=\frac{1}{2}\left[\frac{\partial^2\mathcal{G}_{nj}(\vec{z})}{\partial z_i\partial z_m}+\frac{\partial^2\mathcal{G}_{mj}(\vec{z})}{\partial z_i\partial z_n}\right], \tag{3}$$

and $\mathcal{G}$ is the standard Green tensor satisfying the differential equation of the elasticity theory (Li and Wang, 2008)

$$\mathcal{L}^{(1)}_{ijhk}\frac{\partial^2\mathcal{G}_{hr}(\vec{z})}{\partial z_i\partial z_k}+\delta_{rj}\delta(\vec{z})=0. \tag{4}$$

Here, δ_{rj} is the Kronecker delta and $\delta(\vec{z})$ is the Dirac delta function. It is well known that, when Ω is ellipsoidal, the Eshelby tensor is constant within the inclusion and space-dependent outside it. Therefore, we adopt the notation (see Fig. 2 for details)

$$\mathcal{S}_{nmhk}(\vec{x})=\begin{cases}\mathcal{S}_{nmhk} & \text{if } \vec{x}\in\Omega,\\ \mathcal{S}^{\infty}_{nmhk}(\vec{x}) & \text{if } \vec{x}\notin\Omega.\end{cases} \tag{5}$$

The most important application of the inclusion concept concerns the solution of the inhomogeneity problem through the so-called equivalence principle (Eshelby, 1957, 1959). The inhomogeneity problem consists in finding the perturbation to a uniform elastic field (strain ε^{∞} and stress T^{∞} in a matrix of stiffness $\mathcal{L}^{(1)}$) generated by the presence of an ellipsoidal particle of stiffness $\mathcal{L}^{(2)}$ (see Fig. 3). The approach based on the equivalence principle takes into account the superposition of two configurations (see Fig. 3 for details): a first one A) represented by a homogeneous medium loaded by a remote strain ε^{∞} and a second one B) based on an uniform inclusion with eigenstrain ε^*. Both configurations are based on the same linear elastic matrix $\mathcal{L}^{(1)}$. The solution for

the inhomogeneity problem eventually yields

$$\varepsilon_{tot} = \begin{cases} \mathcal{S}\varepsilon^* + \varepsilon^\infty & \text{if } \vec{x} \in \Omega, \\ \mathcal{S}^\infty(\vec{x})\varepsilon^* + \varepsilon^\infty & \text{if } \vec{x} \notin \Omega, \end{cases} \tag{6}$$

$$T_{tot} = \begin{cases} \mathcal{L}^{(1)}(\mathcal{S}-\mathcal{I})\varepsilon^* + \mathcal{L}^{(1)}\varepsilon^\infty & \text{if } \vec{x} \in \Omega, \\ \mathcal{L}^{(1)}\mathcal{S}^\infty(\vec{x})\varepsilon^* + \mathcal{L}^{(1)}\varepsilon^\infty & \text{if } \vec{x} \notin \Omega. \end{cases} \tag{7}$$

If the inhomogeneity is described by a linear tensor $\mathcal{L}^{(2)}$ we must impose $T_{tot} = \mathcal{L}^{(2)}\varepsilon_{tot}$ within Ω, which corresponds to an equation in ε^*, and then we can easily obtain the constant value of the equivalent eigenstrain

$$\varepsilon^* = \left\{ \left[\mathcal{I} - \left(\mathcal{L}^{(1)}\right)^{-1}\mathcal{L}^{(2)} \right]^{-1} - \mathcal{S} \right\}^{-1} \varepsilon^\infty, \tag{8}$$

and the constant strain induced within the inhomogeneity Ω follows

$$\varepsilon_{tot} = \left\{ \mathcal{I} - \mathcal{S}\left[\mathcal{I} - \left(\mathcal{L}^{(1)}\right)^{-1}\mathcal{L}^{(2)} \right] \right\}^{-1} \varepsilon^\infty. \tag{9}$$

We can generalize this result to the case where the inhomogeneity is nonlinear, i.e. $T_{tot} = \tilde{\mathcal{L}}^{(2)}(\varepsilon_{tot})\varepsilon_{tot}$ within Ω, where $\tilde{\mathcal{L}}^{(2)}(\varepsilon_{tot})$ is any strain-dependent anisotropic stiffness tensor (Giordano et al., 2008, 2009). In order to cope with this problem, we suppose to have found a solution for the equation

$$\varepsilon_{tot} = \left\{ \mathcal{I} - \mathcal{S}\left[\mathcal{I} - \left(\mathcal{L}^{(1)}\right)^{-1}\tilde{\mathcal{L}}^{(2)}(\varepsilon_{tot}) \right] \right\}^{-1} \varepsilon^\infty, \tag{10}$$

obtained from Eq. (9) through the substitution $\mathcal{L}^{(2)} \to \tilde{\mathcal{L}}^{(2)}(\varepsilon_{tot})$. Here, ε_{tot} represents the uniform strain induced inside the nonlinear inhomogeneities. If such a solution exists for a given ε^∞, it means that the nonlinear inhomogeneity could be replaced by a linear one with constant stiffness, without modifications of the elastic fields at any point. Therefore, if the solution exists, then Eq. (10) exactly describes, through self-consistency, the elastic behavior of the nonlinear anisotropic inclusion (Giordano, 2009; Colombo and Giordano, 2011). The existence and unicity of a solution for Eq. (10) can be exactly proved under the sole hypothesis of convexity for the strain energy function of the inhomogeneity (Giordano et al., 2008, 2009).

4. First homogenization: the nonlinear composite ellipsoid

We consider now a second ellipsoidal region Ω_d containing the inhomogeneity Ω ($\Omega_d \supset \Omega$). The definition of this region is purely geometrical and does not affect the elastic properties of the system. Therefore, we have again the elastic tensors $\tilde{\mathcal{L}}^{(2)}$ inside Ω and $\mathcal{L}^{(1)}$ outside it (i.e. in $\Re^3 \backslash \Omega$). The two ellipsoidal regions Ω and Ω_d are completely arbitrary (neither coaxial nor confocal, nor similar) but centred at the same point. The new region Ω_d is useful to properly define the distribution of inhomogeneities within a composite materials characterized by the so-called ellipsoidal microstructure (see Section 2). For the moment, we consider a single nonlinear particle and we suppose to have solved the nonlinear equation stated in Eq. (10). Then, we try to characterize the region Ω_d from the linear and nonlinear elastic point of view. First of all, we determine the average value of $\mathcal{S}^\infty(\vec{x})$ in the external region $\Omega_d \backslash \Omega$

$$\begin{aligned} &\int_{\Omega_d\backslash\Omega} \mathcal{S}^\infty_{nmhk}(\vec{x})d\vec{x} \\ &= -\int_{\Omega_d\backslash\Omega} \mathcal{L}^{(1)}_{ijhk} \int_\Omega \Gamma_{nmij}(\vec{x}-\vec{x}')d\vec{x}'d\vec{x} \\ &= -\int_\Omega \int_{\Omega_d\backslash\Omega} \mathcal{L}^{(1)}_{ijhk}\Gamma_{nmij}(\vec{x}-\vec{x}')d\vec{x}d\vec{x}' \\ &= -\int_\Omega \int_{\Omega_d} \mathcal{L}^{(1)}_{ijhk}\Gamma_{nmij}(\vec{x}-\vec{x}')d\vec{x}d\vec{x}' \\ &\quad + \int_\Omega \int_\Omega \mathcal{L}^{(1)}_{ijhk}\Gamma_{nmij}(\vec{x}-\vec{x}')d\vec{x}d\vec{x}' \\ &= \int_\Omega \left(\mathcal{S}_{d,nmhk} - \mathcal{S}_{nmhk}\right)d\vec{x}', \end{aligned} \tag{11}$$

where $\mathcal{S}_d$ and $\mathcal{S}$ are constant Eshelby tensors corresponding to the ellipsoidal regions Ω_d and Ω, respectively. Therefore, we finally obtain

$$\int_{\Omega_d\backslash\Omega} \mathcal{S}^\infty_{nmhk}(\vec{x})d\vec{x} = v_i\left(\mathcal{S}_{d,nmhk} - \mathcal{S}_{nmhk}\right), \tag{12}$$

where $v_i = \text{mes}(\Omega)$. Incidentally, if Ω and Ω_d are coaxial and similar, then we have that $\mathcal{S}_d = \mathcal{S}$ and we obtain $\int_{\Omega_d\backslash\Omega} \mathcal{S}^\infty(\vec{x})d\vec{x} = 0$, representing the Tanaka–Mori lemma (Tanaka and Mori, 1972; Li and Wang, 2008). In order to evaluate the effective behavior of the region Ω_d, we determine the average values $\langle\varepsilon\rangle_{\Omega_d}$ and $\langle T\rangle_{\Omega_d}$ of strain and stress in this region. For the strain average, we have

$$\begin{aligned} \langle\varepsilon\rangle_{\Omega_d} &= \frac{1}{v_d}\int_\Omega \varepsilon_{tot}d\vec{x} + \frac{1}{v_d}\int_{\Omega_d\backslash\Omega} \varepsilon_{tot}d\vec{x} \\ &= \frac{1}{v_d}\int_\Omega [\mathcal{S}\varepsilon^* + \varepsilon^\infty]d\vec{x} \\ &\quad + \frac{1}{v_d}\int_{\Omega_d\backslash\Omega} [\mathcal{S}^\infty(\vec{x})\varepsilon^* + \varepsilon^\infty]d\vec{x} \\ &= \Phi[\mathcal{S}\varepsilon^* + \varepsilon^\infty] + [\Phi(\mathcal{S}_d - \mathcal{S})\varepsilon^* + (1-\Phi)\varepsilon^\infty] \\ &= \Phi\mathcal{S}_d\varepsilon^* + \varepsilon^\infty, \end{aligned} \tag{13}$$

where we defined $v_d = \text{mes}(\Omega_d)$, $\Phi = v_i/v_d$ and we used Eqs. (6) and (12). On the other hand, for the stress average, we obtain

$$\begin{aligned} \langle T\rangle_{\Omega_d} &= \frac{1}{v_d}\int_\Omega T_{tot}d\vec{x} + \frac{1}{v_d}\int_{\Omega_d\backslash\Omega} T_{tot}d\vec{x} \\ &= \frac{1}{v_d}\int_\Omega \left[\mathcal{L}^{(1)}(\mathcal{S}-\mathcal{I})\varepsilon^* + \mathcal{L}^{(1)}\varepsilon^\infty\right]d\vec{x} \\ &\quad + \frac{1}{v_d}\int_{\Omega_d\backslash\Omega} \left[\mathcal{L}^{(1)}\mathcal{S}^\infty(\vec{x})\varepsilon^* + \mathcal{L}^{(1)}\varepsilon^\infty\right]d\vec{x} \\ &= \Phi\left[\mathcal{L}^{(1)}(\mathcal{S}-\mathcal{I})\varepsilon^* + \mathcal{L}^{(1)}\varepsilon^\infty\right] \\ &\quad + \left[\Phi\mathcal{L}^{(1)}(\mathcal{S}_d - \mathcal{S})\varepsilon^* + (1-\Phi)\mathcal{L}^{(1)}\varepsilon^\infty\right] = \\ &= \Phi\mathcal{L}^{(1)}(\mathcal{S}_d - \mathcal{I})\varepsilon^* + \mathcal{L}^{(1)}\varepsilon^\infty, \end{aligned} \tag{14}$$

where we used Eqs. (7) and (12). Now, the relation between ε^* and ε^∞ can be written as

$$\varepsilon^* = \left\{ \left[\mathcal{I} - \left(\mathcal{L}^{(1)}\right)^{-1}\tilde{\mathcal{L}}^{(2)} \right]^{-1} - \mathcal{S} \right\}^{-1} \varepsilon^\infty \triangleq \tilde{\mathcal{B}}\varepsilon^\infty, \tag{15}$$

representing the nonlinear generalization of Eq. (8). We can therefore rewrite Eqs. (13) and (14) by taking into account Eq. (15)

$$\langle\varepsilon\rangle_{\Omega_d} = \left[\mathcal{I} + \Phi\mathcal{S}_d\tilde{\mathcal{B}}\right]\varepsilon^\infty, \tag{16}$$

$$\langle T\rangle_{\Omega_d} = \mathcal{L}^{(1)}\left[\mathcal{I} + \Phi(\mathcal{S}_d - \mathcal{I})\tilde{\mathcal{B}}\right]\varepsilon^\infty. \tag{17}$$

These exact results allow us to determine the relationship between $\langle T\rangle_{\Omega_d}$ and $\langle\varepsilon\rangle_{\Omega_d}$. Indeed, by eliminating ε^∞ in previous relations, we obtain the equivalent constitutive equation for the region Ω_d

$$\begin{aligned} \langle T\rangle_{\Omega_d} &= \mathcal{L}^{(1)}\left[\mathcal{I} + \Phi\mathcal{S}_d\tilde{\mathcal{B}} - \mathcal{I}\tilde{\mathcal{B}}\right]\left[\mathcal{I} + \Phi\mathcal{S}_d\tilde{\mathcal{B}}\right]^{-1}\langle\varepsilon\rangle_{\Omega_d} \\ &= \mathcal{L}^{(1)}\langle\varepsilon\rangle_{\Omega_d} - \Phi\mathcal{L}^{(1)}\left[\tilde{\mathcal{B}}^{-1} + \Phi\mathcal{S}_d\right]^{-1}\langle\varepsilon\rangle_{\Omega_d}. \end{aligned} \tag{18}$$

By using the definition of $\tilde{\mathcal{B}}$ given in Eq. (15), we eventually obtain

$$\langle T\rangle_{\Omega_d} = \left\{\mathcal{L}^{(1)} + \Phi\left[\tilde{\mathcal{L}}^{(2)} - \mathcal{L}^{(1)}\right]\tilde{\mathcal{A}}^{-1}\right\}\langle\varepsilon\rangle_{\Omega_d}, \tag{19}$$

where we defined

$$\tilde{\mathcal{A}} = \mathcal{I} - (\mathcal{S} - \Phi\mathcal{S}_d)\left[\mathcal{I} - \left(\mathcal{L}^{(1)}\right)^{-1}\tilde{\mathcal{L}}^{(2)}\right]. \tag{20}$$

It is important to remark that we are working with a nonlinear inhomogeneity and therefore we must consider $\tilde{\mathcal{L}}^{(2)} = \tilde{\mathcal{L}}^{(2)}(\varepsilon_{tot})$. It means that into Eqs. (19) and (20) we must substitute the relation $\varepsilon_{tot} = \varepsilon_{tot}(\langle\varepsilon\rangle_{\Omega_d})$, for obtaining the nonlinear constitutive equation (see Eq. (19)), linking $\langle T\rangle_{\Omega_d}$ and $\langle\varepsilon\rangle_{\Omega_d}$. In order to find the implicit dependence $\varepsilon_{tot} = \varepsilon_{tot}(\langle\varepsilon\rangle_{\Omega_d})$, we can use the following system of equations based on Eqs. (6) and (7) for $\vec{x}\in\Omega$ and Eq. (13) for $\langle\varepsilon\rangle_{\Omega_d}$

$$\varepsilon_{tot} = \mathcal{S}\varepsilon^* + \varepsilon^\infty, \tag{21}$$

$$T_{tot} = \tilde{\mathcal{L}}^{(2)}(\varepsilon_{tot})\varepsilon_{tot} = \mathcal{L}^{(1)}(\mathcal{S} - \mathcal{I})\varepsilon^* + \mathcal{L}^{(1)}\varepsilon^\infty, \tag{22}$$

$$\langle\varepsilon\rangle_{\Omega_d} = \Phi\mathcal{S}_d\varepsilon^* + \varepsilon^\infty. \tag{23}$$

By determining ε^∞ from the first equation and substituting it into the other ones, we get

$$\tilde{\mathcal{L}}^{(2)}(\varepsilon_{tot})\varepsilon_{tot} = \mathcal{L}^{(1)}(\mathcal{S} - \mathcal{I})\varepsilon^* + \mathcal{L}^{(1)}(\varepsilon_{tot} - \mathcal{S}\varepsilon^*), \tag{24}$$

$$\langle\varepsilon\rangle_{\Omega_d} = \Phi\mathcal{S}_d\varepsilon^* + \varepsilon_{tot} - \mathcal{S}\varepsilon^*. \tag{25}$$

Further, by eliminating ε^*, we obtain the requested relation between ε_{tot} and $\langle\varepsilon\rangle_{\Omega_d}$ in the implicit form

$$\left\{\mathcal{I} - (\mathcal{S} - \Phi\mathcal{S}_d)\left[\mathcal{I} - \left(\mathcal{L}^{(1)}\right)^{-1}\tilde{\mathcal{L}}^{(2)}(\varepsilon_{tot})\right]\right\}\varepsilon_{tot} = \langle\varepsilon\rangle_{\Omega_d}, \tag{26}$$

or, equivalently, in the simplified form $\tilde{\mathcal{A}}\varepsilon_{tot} = \langle\varepsilon\rangle_{\Omega_d}$. The elastic behavior of the region Ω_d is therefore summed-up by the nonlinear constitutive equation

$$\langle T\rangle_{\Omega_d} = \mathcal{L}^{(1)}\langle\varepsilon\rangle_{\Omega_d} + \Phi\left[\tilde{\mathcal{L}}^{(2)}(\varepsilon_{tot}) - \mathcal{L}^{(1)}\right]\varepsilon_{tot}, \tag{27}$$

$$\tilde{\mathcal{A}}\varepsilon_{tot} = \langle\varepsilon\rangle_{\Omega_d}, \tag{28}$$

coming from Eqs. (19)and (26) and where $\tilde{\mathcal{A}}$ is given in Eq. (20). Once solved Eq. (28) for ε_{tot}, the solution can be substituted in Eq. (27) giving the overall behavior of Ω_d. We underline that this result is exact, i.e. not affected by any form of approximation. In particular, it is valid for any value of the volume fraction Φ in the entire range $0 < \Phi < 1$. Moreover, it is valid for any strain-dependent and anisotropic stiffness tensor $\tilde{\mathcal{L}}^{(2)}(\varepsilon_{tot})$, describing the nonlinear particle elasticity. In the next section, we specialize this result to a second order constitutive equation.

4.1. Second order constitutive equation

In order to show an explicit application of the previous theory, we consider for the inhomogeneity a nonlinear constitutive equation expanded up to the second order in the strain

$$\tilde{\mathcal{L}}^{(2)}(\varepsilon_{tot}) = \mathcal{L}^{(2)} + \mathcal{N}^{(2)}\varepsilon_{tot}, \tag{29}$$

which means, by explicitly considering the tensor components, $\tilde{\mathcal{L}}^{(2)}_{ijhk}(\varepsilon_{tot}) = \mathcal{L}^{(2)}_{ijhk} + \mathcal{N}^{(2)}_{ijhknm}\varepsilon_{tot,nm}$. Here, $\mathcal{N}^{(2)}$ is the tensor describing the nonlinear properties of the inhomogeneity. It follows that Eq. (28) assumes the form

$$\mathcal{A}\varepsilon_{tot} + (\mathcal{S} - \Phi\mathcal{S}_d)\left(\mathcal{L}^{(1)}\right)^{-1}\mathcal{N}^{(2)}\varepsilon_{tot}\varepsilon_{tot} = \langle\varepsilon\rangle_{\Omega_d}, \tag{30}$$

where

$$\mathcal{A} = \mathcal{I} - (\mathcal{S} - \Phi\mathcal{S}_d)\left[\mathcal{I} - \left(\mathcal{L}^{(1)}\right)^{-1}\mathcal{L}^{(2)}\right]. \tag{31}$$

The latter represents the simplified counterpart of Eq. (20), where $\tilde{\mathcal{L}}^{(2)}$ is substituted by $\mathcal{L}^{(2)}$. The product $\mathcal{N}^{(2)}\varepsilon_{tot}\varepsilon_{tot}$ in Eq. (30) represents the operation $(\mathcal{N}^{(2)}\varepsilon_{tot}\varepsilon_{tot})_{ij} = \mathcal{N}^{(2)}_{ijhknm}\varepsilon_{tot,hk}\varepsilon_{tot,nm}$. In order to solve Eq. (30), we search for a solution in the form $\varepsilon_{tot} = \mathcal{C}\langle\varepsilon\rangle_{\Omega_d} + \mathcal{D}\langle\varepsilon\rangle_{\Omega_d}\langle\varepsilon\rangle_{\Omega_d}$, representing a second order expansion in the average strain. By substituting this guess into Eq. (30), and retaining only the terms up to the second order in $\langle\varepsilon\rangle_{\Omega_d}$ we get

$$\begin{aligned}&\mathcal{A}\mathcal{C}\langle\varepsilon\rangle_{\Omega_d} + \mathcal{A}\mathcal{D}\langle\varepsilon\rangle_{\Omega_d}\langle\varepsilon\rangle_{\Omega_d} \\ &\quad + (\mathcal{S} - \Phi\mathcal{S}_d)\left(\mathcal{L}^{(1)}\right)^{-1}\mathcal{N}^{(2)}\left(\mathcal{C}\langle\varepsilon\rangle_{\Omega_d}\right)\left(\mathcal{C}\langle\varepsilon\rangle_{\Omega_d}\right) = \langle\varepsilon\rangle_{\Omega_d}.\end{aligned} \tag{32}$$

The product $\mathcal{N}^{(2)}\left(\mathcal{C}\langle\varepsilon\rangle_{\Omega_d}\right)\left(\mathcal{C}\langle\varepsilon\rangle_{\Omega_d}\right)$ must be interpreted as follows: $\left[\mathcal{N}^{(2)}\left(\mathcal{C}\langle\varepsilon\rangle_{\Omega_d}\right)\left(\mathcal{C}\langle\varepsilon\rangle_{\Omega_d}\right)\right]_{ij} = \mathcal{N}^{(2)}_{ijkhrs}\mathcal{C}_{khnm}\langle\varepsilon\rangle_{\Omega_d,nm}\mathcal{C}_{rspq}\langle\varepsilon\rangle_{\Omega_d,pq} = \left[\mathcal{N}^{(2)}\mathcal{C}\mathcal{C}\langle\varepsilon\rangle_{\Omega_d}\langle\varepsilon\rangle_{\Omega_d}\right]_{ij}$ where $\left[\mathcal{N}^{(2)}\mathcal{C}\mathcal{C}\right]_{ijnmpq} = \mathcal{N}^{(2)}_{ijkhrs}\mathcal{C}_{khnm}\mathcal{C}_{rspq}$. It follows that Eq. (32) is equivalent to $\mathcal{A}\mathcal{C} = \mathcal{I}$ and $\mathcal{A}\mathcal{D} + \mathcal{N}^{(2)}\mathcal{C}\mathcal{C} = 0$. Summing up, we easily obtain the tensor quantities $\mathcal{C}$ and $\mathcal{D}$ and we can write ε_{tot} in terms of $\langle\varepsilon\rangle_{\Omega_d}$ as follows

$$\begin{aligned}\varepsilon_{tot} &= \mathcal{A}^{-1}\langle\varepsilon\rangle_{\Omega_d} \\ &\quad -\mathcal{A}^{-1}(\mathcal{S} - \Phi\mathcal{S}_d)\left(\mathcal{L}^{(1)}\right)^{-1}\mathcal{N}^{(2)}\mathcal{A}^{-1}\mathcal{A}^{-1}\langle\varepsilon\rangle_{\Omega_d}\langle\varepsilon\rangle_{\Omega_d}.\end{aligned} \tag{33}$$

To conclude, we can substitute Eq. (33) into Eq. (27), eventually yielding the nonlinear constitutive equation of the region Ω_d

$$\begin{aligned}\langle T\rangle_{\Omega_d} &= \left[\mathcal{L}^{(1)} + \Phi\left(\mathcal{L}^{(2)} - \mathcal{L}^{(1)}\right)\mathcal{A}^{-1}\right]\langle\varepsilon\rangle_{\Omega_d} \\ &\quad + \Phi\left[\mathcal{I} - \left(\mathcal{L}^{(2)} - \mathcal{L}^{(1)}\right)\mathcal{A}^{-1}(\mathcal{S} - \Phi\mathcal{S}_d)\left(\mathcal{L}^{(1)}\right)^{-1}\right] \\ &\quad \times\mathcal{N}^{(2)}\mathcal{A}^{-1}\mathcal{A}^{-1}\langle\varepsilon\rangle_{\Omega_d}\langle\varepsilon\rangle_{\Omega_d}.\end{aligned} \tag{34}$$

This is the final exact result expanded up to the second order in the overall strain, where $\mathcal{A}$ is given in Eq. (31). The higher order terms are not considered here since we are interested in the second order homogenization. Nevertheless, the exposed techniques can be adopted to determine any needed term in the expansion. Eq. (34) can be also summarized by identifying the linear effective properties

$$\mathcal{L}^{(d)} = \mathcal{L}^{(1)} + \Phi\left(\mathcal{L}^{(2)} - \mathcal{L}^{(1)}\right)\mathcal{A}^{-1}, \tag{35}$$

and the nonlinear effective properties

$$\begin{aligned}\mathcal{N}^{(d)} &= \Phi\left[\mathcal{I} - \left(\mathcal{L}^{(2)} - \mathcal{L}^{(1)}\right)\mathcal{A}^{-1}(\mathcal{S} - \Phi\mathcal{S}_d)\left(\mathcal{L}^{(1)}\right)^{-1}\right] \\ &\quad \times\mathcal{N}^{(2)}\mathcal{A}^{-1}\mathcal{A}^{-1},\end{aligned} \tag{36}$$

pertaining to the region Ω_d. It is useful to remember that this result is valid for any value of the volume fraction Φ in the entire range $0 < \Phi < 1$.

5. Second homogenization: the dispersion of nonlinear inhomogeneities

Now, we take into consideration a population of parallel ellipsoidal inhomogeneities described by the arbitrary strain-dependent elastic tensor $\tilde{\mathcal{L}}^{(d)}(\varepsilon_d)$ embedded in the linear matrix with constant stiffness $\mathcal{L}^{(1)}$. The shape of each ellipsoidal particle is represented by the Eshelby tensor $\mathcal{S}_d$. Moreover, we suppose to deal with a dilute distribution characterized by the volume fraction Ψ. If we apply a remote strain ε^∞ to the system, the internal strain in a given particle is implicitly given by the equation

$$\varepsilon_d = \left\{\mathcal{I} - \mathcal{S}_d\left[\mathcal{I} - \left(\mathcal{L}^{(1)}\right)^{-1}\tilde{\mathcal{L}}^{(d)}(\varepsilon_d)\right]\right\}^{-1}\varepsilon^\infty, \tag{37}$$

coming from Eq. (10). Indeed, because of the small volume fraction Ψ, the interactions among inhomogeneities can be neglected in the calculation of the internal strain ε_d. If we consider, as before, a second order nonlinear constitutive equation given by $T_d = \tilde{\mathcal{L}}^{(d)}(\varepsilon_d)\varepsilon_d = \mathcal{L}^{(d)}\varepsilon_d + \mathcal{N}^{(d)}\varepsilon_d\varepsilon_d$, we get from Eq. (37)

$$\left\{\mathcal{I}-\mathcal{S}_d\left[\mathcal{I}-\left(\mathcal{L}^{(1)}\right)^{-1}\mathcal{L}^{(d)}\right]\right\}\varepsilon_d + \mathcal{S}_d\left(\mathcal{L}^{(1)}\right)^{-1}\mathcal{N}^{(d)}\varepsilon_d\varepsilon_d = \varepsilon^{\infty}. \tag{38}$$

To homogenize the overall system, we generalize the classical Mori–Tanaka scheme in order to consider the second order nonlinear behavior. To this aim we determine the average strain tensor within the structure through the simple weighted mean

$$\langle\varepsilon\rangle_{\Upsilon} = \Psi\varepsilon_d + (1-\Psi)\varepsilon^{\infty}, \tag{39}$$

over the whole region $\Upsilon = \Gamma \bigcup \Delta$, composed of matrix (region Γ) and particles (region Δ). Of course, this approximation is valid under the hypothesis of small volume fraction Ψ. On the other hand, we can determine the average stress tensor as follows

$$\begin{aligned}\langle T\rangle_{\Upsilon} &= \frac{1}{v}\int_{\Upsilon} T d\vec{x} = \frac{1}{v}\mathcal{L}^{(1)}\int_{\Gamma}\varepsilon d\vec{x} + \frac{1}{v}\int_{\Delta} T d\vec{x}\\ &= \frac{1}{v}\mathcal{L}^{(1)}\int_{\Gamma}\varepsilon d\vec{x} + \frac{1}{v}\int_{\Delta} T d\vec{x}\\ &\quad + \frac{1}{v}\mathcal{L}^{(1)}\int_{\Delta}\varepsilon d\vec{x} - \frac{1}{v}\mathcal{L}^{(1)}\int_{\Delta}\varepsilon d\vec{x}\\ &= \frac{1}{v}\mathcal{L}^{(1)}\int_{\Upsilon}\varepsilon d\vec{x} + \frac{1}{v}\int_{\Delta}\left(T - \mathcal{L}^{(1)}\varepsilon\right)d\vec{x}\\ &= \mathcal{L}^{(1)}\langle\varepsilon\rangle_{\Upsilon} + \Psi\left(T_d - \mathcal{L}^{(1)}\varepsilon_d\right),\end{aligned} \tag{40}$$

where we defined $v = \mathrm{mes}(\Upsilon)$. The averages in Eqs. (39) and (40) can be rewritten by taking into account the second order constitutive equation of the particles and Eq. (38)

$$\langle\varepsilon\rangle_{\Upsilon} = \mathcal{A}_d\varepsilon_d + (1-\Psi)\mathcal{S}_d\left(\mathcal{L}^{(1)}\right)^{-1}\mathcal{N}^{(d)}\varepsilon_d\varepsilon_d, \tag{41}$$

$$\langle T\rangle_{\Upsilon} = \mathcal{L}^{(1)}\langle\varepsilon\rangle_{\Upsilon} + \Psi\left[(\mathcal{L}^{(d)} - \mathcal{L}^{(1)})\varepsilon_d + \mathcal{N}^{(d)}\varepsilon_d\varepsilon_d\right], \tag{42}$$

where

$$\begin{aligned}\mathcal{A}_d &= \Psi\mathcal{I} + (1-\Psi)\left\{\mathcal{I} - \mathcal{S}_d\left[\mathcal{I} - \left(\mathcal{L}^{(1)}\right)^{-1}\mathcal{L}^{(d)}\right]\right\}\\ &= \mathcal{I} - (1-\Psi)\mathcal{S}_d\left[\mathcal{I} - \left(\mathcal{L}^{(1)}\right)^{-1}\mathcal{L}^{(d)}\right].\end{aligned} \tag{43}$$

The combination of Eqs. (41) and (42) gives the characterization of the composite material. Indeed, we can invert Eq. (41) to get ε_d in terms of $\langle\varepsilon\rangle_{\Upsilon}$

$$\begin{aligned}\varepsilon_d &= \mathcal{A}_d^{-1}\langle\varepsilon\rangle_{\Upsilon}\\ &\quad - (1-\Psi)\mathcal{A}_d^{-1}\mathcal{S}_d\left(\mathcal{L}^{(1)}\right)^{-1}\mathcal{N}^{(d)}\mathcal{A}_d^{-1}\mathcal{A}_d^{-1}\langle\varepsilon\rangle_{\Upsilon}\langle\varepsilon\rangle_{\Upsilon}.\end{aligned} \tag{44}$$

Of course, this expression represents the expansion of ε_d up to the second order in $\langle\varepsilon\rangle_{\Upsilon}$. Then, we can substitute Eq. (44) into Eq. (42), eventually obtaining the following effective nonlinear constitutive equation

$$\begin{aligned}\langle T\rangle_{\Upsilon} &= \left[\mathcal{L}^{(1)} + \Psi\left(\mathcal{L}^{(d)} - \mathcal{L}^{(1)}\right)\mathcal{A}_d^{-1}\right]\langle\varepsilon\rangle_{\Upsilon}\\ &\quad + \Psi\left[\mathcal{I} - (1-\Psi)\left(\mathcal{L}^{(d)} - \mathcal{L}^{(1)}\right)\mathcal{A}_d^{-1}\mathcal{S}_d\left(\mathcal{L}^{(1)}\right)^{-1}\right]\\ &\quad \times\mathcal{N}^{(d)}\mathcal{A}_d^{-1}\mathcal{A}_d^{-1}\langle\varepsilon\rangle_{\Upsilon}\langle\varepsilon\rangle_{\Upsilon}.\end{aligned} \tag{45}$$

This is the homogenization result expanded up to the second order in the overall strain. Eq. (45) corresponds to the linear effective tensor

$$\mathcal{L}^{(eff)} = \mathcal{L}^{(1)} + \Psi\left(\mathcal{L}^{(d)} - \mathcal{L}^{(1)}\right)\mathcal{A}_d^{-1}, \tag{46}$$

and to the nonlinear effective tensor

$$\begin{aligned}\mathcal{N}^{(eff)} &= \Psi\left[\mathcal{I} - (1-\Psi)\left(\mathcal{L}^{(d)} - \mathcal{L}^{(1)}\right)\mathcal{A}_d^{-1}\mathcal{S}_d\left(\mathcal{L}^{(1)}\right)^{-1}\right]\\ &\quad\times\mathcal{N}^{(d)}\mathcal{A}_d^{-1}\mathcal{A}_d^{-1},\end{aligned} \tag{47}$$

pertaining to the whole region Y. While the linear result stated in Eq. (46) is in perfect agreement with the Mori and Tanaka's (1973) scheme, the nonlinear tensor given in Eq. (47) is a new achievement. Nevertheless, if we consider the particular case of a dispersion of isotropic nonlinear spheres in an isotropic linear matrix, Eq. (47) gives specific results already discussed in the literature (Giordano et al., 2008, 2009; Giordano, 2009; Colombo and Giordano, 2011).

6. Results for the ellipsoidal microstructure

In this section we combine the two homogenization procedures above proposed, in order to determine the linear and nonlinear effective properties of the composite material with ellipsoidal microstructure. This approach, based on a multiscale approach, is summarized in Fig. 4, where we can observe the two-level multiscale paradigm applied to the present problem.

We underline the different character of the two steps involved in the procedure: while the first homogenization is based on an exact result for a single composite particle, the second one is an approximation valid only for small volume fractions of the dispersion of particles. If we combine the two schemes, we finally obtain a composite material with a real volume fraction $c = \frac{Nv_i}{v} = \Phi\Psi$ of the dispersed phase in the matrix. In principle, the final result concerning the nonlinear homogenization can be obtained by simply substituting Eqs. (35) and (36) in Eqs. (46) and (47). Nevertheless, this calculation reveals non-trivial algebraic issues.

We start the calculation by considering the linear response. The direct calculation yields

$$\begin{aligned}\mathcal{L}^{(eff)} &= \mathcal{L}^{(1)} + \Psi\left(\mathcal{L}^{(d)} - \mathcal{L}^{(1)}\right)\mathcal{A}_d^{-1}\\ &= \mathcal{L}^{(1)} + \Psi\left(\mathcal{L}^{(d)} - \mathcal{L}^{(1)}\right)\left\{\mathcal{I} - (1-\Psi)\mathcal{S}_d\right.\\ &\quad\left.\times\left[\mathcal{I} - \left(\mathcal{L}^{(1)}\right)^{-1}\mathcal{L}^{(d)}\right]\right\}^{-1}\\ &= \mathcal{L}^{(1)} + \Psi\left\{\left(\mathcal{L}^{(d)} - \mathcal{L}^{(1)}\right)^{-1}\right.\\ &\quad\left. + (1-\Psi)\mathcal{S}_d\left(\mathcal{L}^{(1)}\right)^{-1}\right\}^{-1}\\ &= \mathcal{L}^{(1)} + \Psi\left\{\Phi^{-1}\mathcal{A}\left(\mathcal{L}^{(2)} - \mathcal{L}^{(1)}\right)^{-1}\right.\\ &\quad\left. + (1-\Psi)\mathcal{S}_d\left(\mathcal{L}^{(1)}\right)^{-1}\right\}^{-1}\\ &= \mathcal{L}^{(1)} + \Psi\left\{\Phi^{-1}\left(\mathcal{L}^{(2)} - \mathcal{L}^{(1)}\right)^{-1}\right.\\ &\quad + \Phi^{-1}(\mathcal{S} - \Phi\mathcal{S}_d)\left(\mathcal{L}^{(1)}\right)^{-1}\\ &\quad\left. + (1-\Psi)\mathcal{S}_d\left(\mathcal{L}^{(1)}\right)^{-1}\right\}^{-1}\\ &= \mathcal{L}^{(1)} + \Psi\Phi\left\{\left(\mathcal{L}^{(2)} - \mathcal{L}^{(1)}\right)^{-1} + \mathcal{S}\left(\mathcal{L}^{(1)}\right)^{-1}\right.\\ &\quad\left. - \Psi\Phi\mathcal{S}_d\left(\mathcal{L}^{(1)}\right)^{-1}\right\}^{-1}\\ &= \mathcal{L}^{(1)} + c\left(\mathcal{L}^{(2)} - \mathcal{L}^{(1)}\right)\mathcal{A}_{eff}^{-1},\end{aligned} \tag{48}$$

where we defined

$$\mathcal{A}_{eff} = \mathcal{I} - (\mathcal{S} - c\mathcal{S}_d)\left[\mathcal{I} - \left(\mathcal{L}^{(1)}\right)^{-1}\mathcal{L}^{(2)}\right]. \tag{49}$$

To develop Eq. (48), we used the definitions of tensors $\mathcal{A}$ and $\mathcal{A}_d$, given in Eqs. (31) and (43), respectively.

The calculation concerning the nonlinear response is more involved. To begin, we substitute Eq. (36) in Eq. (47), getting

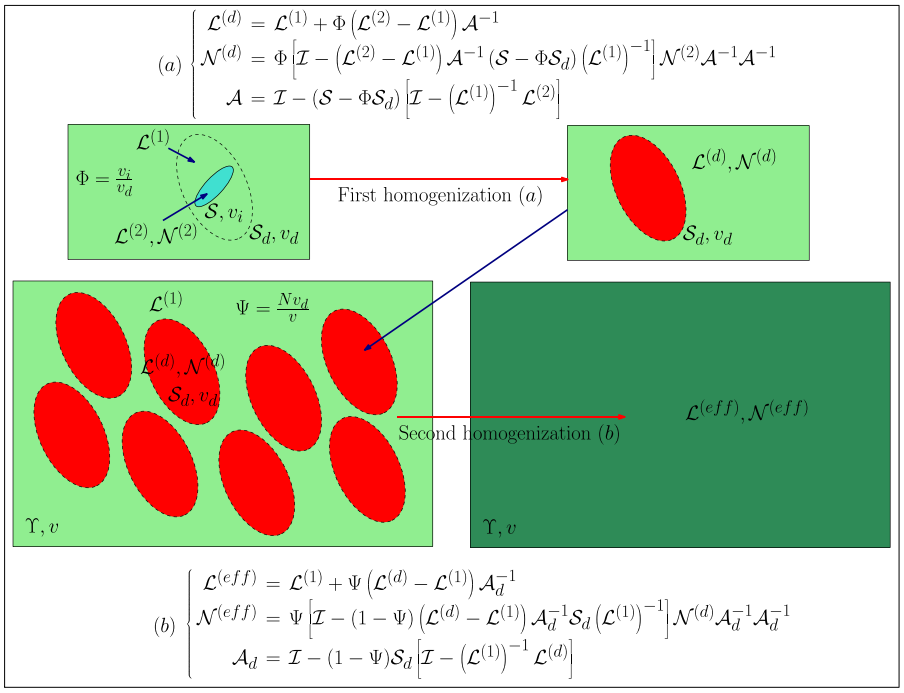

Fig. 4. Distribution of particles embedded in the matrix $\mathcal{L}^{(1)}$ showing the so-called ellipsoidal microstructure. Each nonlinear inhomogeneity is characterized by an ellipsoidal region Ω, a volume $v_i = \text{mes}(\Omega)$, an Eshelby tensor $\mathcal{S}$ and a strain-dependent stiffness tensor $\tilde{\mathcal{L}}^{(2)}(\varepsilon_{tot})$. Moreover, every particle is surrounded by another ellipsoidal region Ω_d having volume v_d and Eshelby tensor $\mathcal{S}_d$.

$$\begin{aligned}\mathcal{N}^{(eff)} &= \Psi\Phi \\ &\times \left[\mathcal{I} - (1-\Psi)\left(\mathcal{L}^{(d)} - \mathcal{L}^{(1)}\right)\mathcal{A}_d^{-1}\mathcal{S}_d\left(\mathcal{L}^{(1)}\right)^{-1}\right] \\ &\times \left[\mathcal{I} - \left(\mathcal{L}^{(2)} - \mathcal{L}^{(1)}\right)\mathcal{A}^{-1}\left(\mathcal{S} - \Phi\mathcal{S}_d\right)\left(\mathcal{L}^{(1)}\right)^{-1}\right] \\ &\times \mathcal{N}^{(2)}\left(\mathcal{A}^{-1}\mathcal{A}_d^{-1}\right)\left(\mathcal{A}^{-1}\mathcal{A}_d^{-1}\right). \end{aligned} \tag{50}$$

We analyse now the product $\mathcal{A}^{-1}\mathcal{A}_d^{-1}$. From Eq. (35) we easily find

$$\mathcal{A}^{-1} = \frac{1}{\Phi}\left(\mathcal{L}^{(2)} - \mathcal{L}^{(1)}\right)^{-1}\left(\mathcal{L}^{(d)} - \mathcal{L}^{(1)}\right). \tag{51}$$

Similarly, by comparing the first and the last line in Eq. (48), we have

$$\mathcal{A}_d^{-1} = \Phi\left(\mathcal{L}^{(d)} - \mathcal{L}^{(1)}\right)^{-1}\left(\mathcal{L}^{(2)} - \mathcal{L}^{(1)}\right)\mathcal{A}_{eff}^{-1}. \tag{52}$$

Hence, by multiplying Eqs. (51) and (52), we obtain the important relation

$$\mathcal{A}^{-1}\mathcal{A}_d^{-1} = \mathcal{A}_{eff}^{-1}. \tag{53}$$

Therefore, the nonlinear effective tensor can be rewritten as

$$\begin{aligned}\mathcal{N}^{(eff)} &= \Psi\Phi \\ &\times \left[\mathcal{I} - (1-\Psi)\Phi\left(\mathcal{L}^{(2)} - \mathcal{L}^{(1)}\right)\mathcal{A}_{eff}^{-1}\mathcal{S}_d\left(\mathcal{L}^{(1)}\right)^{-1}\right] \\ &\times \left[\mathcal{I} - \left(\mathcal{L}^{(2)} - \mathcal{L}^{(1)}\right)\mathcal{A}^{-1}\left(\mathcal{S} - \Phi\mathcal{S}_d\right)\left(\mathcal{L}^{(1)}\right)^{-1}\right] \\ &\times \mathcal{N}^{(2)}\mathcal{A}_{eff}^{-1}\mathcal{A}_{eff}^{-1}, \end{aligned} \tag{54}$$

where $\left(\mathcal{L}^{(d)} - \mathcal{L}^{(1)}\right)\mathcal{A}_d^{-1}$ in the first square brackets has been substituted with $\Phi\left(\mathcal{L}^{(2)} - \mathcal{L}^{(1)}\right)\mathcal{A}_{eff}^{-1}$, according to Eq. (52). The second square brackets term can be elaborated with the following tensor property

$$(\mathcal{I} + \mathcal{Y}\mathcal{X})^{-1} = \mathcal{I} - \mathcal{Y}(\mathcal{I} + \mathcal{X}\mathcal{Y})^{-1}\mathcal{X}, \tag{55}$$

which is valid when $\mathcal{I} + \mathcal{X}\mathcal{Y}$ and $\mathcal{I} + \mathcal{Y}\mathcal{X}$ are non-singular. First of all, we can prove this property by directly multiplying $\mathcal{I} - \mathcal{Y}(\mathcal{I} + \mathcal{X}\mathcal{Y})^{-1}\mathcal{X}$ and $\mathcal{I} + \mathcal{Y}\mathcal{X}$, as follows

$$\begin{aligned}&\left[\mathcal{I} - \mathcal{Y}(\mathcal{I} + \mathcal{X}\mathcal{Y})^{-1}\mathcal{X}\right](\mathcal{I} + \mathcal{Y}\mathcal{X}) \\ &= \mathcal{I} + \mathcal{Y}\mathcal{X} - \mathcal{Y}(\mathcal{I} + \mathcal{X}\mathcal{Y})^{-1}\mathcal{X} - \mathcal{Y}(\mathcal{I} + \mathcal{X}\mathcal{Y})^{-1}\mathcal{X}\mathcal{Y}\mathcal{X} \\ &= \mathcal{I} + \mathcal{Y}\mathcal{X} - \mathcal{Y}(\mathcal{I} + \mathcal{X}\mathcal{Y})^{-1}(\mathcal{I} + \mathcal{X}\mathcal{Y})\mathcal{X} = \mathcal{I}. \end{aligned} \tag{56}$$

Then, we can elaborate Eq. (54) by considering the expression $\mathcal{A} = \mathcal{I} + (\mathcal{S} - \Phi\mathcal{S}_d)\left(\mathcal{L}^{(1)}\right)^{-1}\left(\mathcal{L}^{(2)} - \mathcal{L}^{(1)}\right)$ (see Eq. (31)). Indeed, if we take account of this expression, the second square brackets term of Eq. (54) assumes the form $\mathcal{I} - \mathcal{Y}(\mathcal{I} + \mathcal{X}\mathcal{Y})^{-1}\mathcal{X}$ where $\mathcal{X} = (\mathcal{S} - \Phi\mathcal{S}_d)\left(\mathcal{L}^{(1)}\right)^{-1}$ and $\mathcal{Y} = \mathcal{L}^{(2)} - \mathcal{L}^{(1)}$. It is true since $\mathcal{A}$ takes the simple form $\mathcal{I} + \mathcal{X}\mathcal{Y}$. Hence, the second square brackets term of Eq. (54), according to Eq. (55), can be finally written as $(\mathcal{I} + \mathcal{Y}\mathcal{X})^{-1}$ and we get

$$\mathcal{N}^{(eff)} = \Psi\Phi\mathcal{E}\mathcal{G}^{-1}\mathcal{N}^{(2)}\mathcal{A}_{eff}^{-1}\mathcal{A}_{eff}^{-1}, \tag{57}$$

where we introduced

$$\mathcal{E} = \mathcal{I} - (1-\Psi)\Phi\left(\mathcal{L}^{(2)} - \mathcal{L}^{(1)}\right)\mathcal{A}_{eff}^{-1}\mathcal{S}_d\left(\mathcal{L}^{(1)}\right)^{-1}, \tag{58}$$

$$\mathcal{G} = \mathcal{I} + \left(\mathcal{L}^{(2)} - \mathcal{L}^{(1)}\right)\left(\mathcal{S} - \Phi\mathcal{S}_d\right)\left(\mathcal{L}^{(1)}\right)^{-1}. \tag{59}$$

We can now prove that the product $\mathcal{F} = \mathcal{E}\mathcal{G}^{-1}$ can be performed by eventually obtaining

$$\mathcal{F} = \mathcal{I} - \left(\mathcal{L}^{(2)} - \mathcal{L}^{(1)}\right)\mathcal{A}_{eff}^{-1}\left(\mathcal{S} - c\mathcal{S}_d\right)\left(\mathcal{L}^{(1)}\right)^{-1}. \tag{60}$$

To prove this statement, we calculate $\mathcal{F}\mathcal{G} - \mathcal{E}$ as follows

$$\begin{aligned}\mathcal{F}\mathcal{G} - \mathcal{E} = &\Phi\left(\mathcal{L}^{(2)} - \mathcal{L}^{(1)}\right)\mathcal{A}_{eff}^{-1}\mathcal{S}_d\left(\mathcal{L}^{(1)}\right)^{-1} \\ &+ \left(\mathcal{L}^{(2)} - \mathcal{L}^{(1)}\right)\left(\mathcal{S} - \Phi\mathcal{S}_d\right)\left(\mathcal{L}^{(1)}\right)^{-1} \\ &- \left(\mathcal{L}^{(2)} - \mathcal{L}^{(1)}\right)\mathcal{A}_{eff}^{-1}\mathcal{S}\left(\mathcal{L}^{(1)}\right)^{-1} \\ &- \left(\mathcal{L}^{(2)} - \mathcal{L}^{(1)}\right)\mathcal{A}_{eff}^{-1}\left(\mathcal{S} - c\mathcal{S}_d\right)\left(\mathcal{L}^{(1)}\right)^{-1} \\ &\times\left(\mathcal{L}^{(2)} - \mathcal{L}^{(1)}\right)\left(\mathcal{S} - \Phi\mathcal{S}_d\right)\left(\mathcal{L}^{(1)}\right)^{-1} \end{aligned}$$

$$= \left(\mathcal{L}^{(2)} - \mathcal{L}^{(1)}\right)\left[\mathcal{I} - \mathcal{A}_{eff}^{-1} - \mathcal{A}_{eff}^{-1}(\mathcal{S} - c\mathcal{S}_d)\right.$$
$$\left.\times\left(\mathcal{L}^{(1)}\right)^{-1}\left(\mathcal{L}^{(2)} - \mathcal{L}^{(1)}\right)\right](\mathcal{S} - \Phi\mathcal{S}_d)\left(\mathcal{L}^{(1)}\right)^{-1}$$
$$= \left(\mathcal{L}^{(2)} - \mathcal{L}^{(1)}\right)\left\{\mathcal{I} - \mathcal{A}_{eff}^{-1}\right.$$
$$\left.\times\left[\mathcal{I} + (\mathcal{S} - c\mathcal{S}_d)\left(\mathcal{L}^{(1)}\right)^{-1}\left(\mathcal{L}^{(2)} - \mathcal{L}^{(1)}\right)\right]\right\}$$
$$\times(\mathcal{S} - \Phi\mathcal{S}_d)\left(\mathcal{L}^{(1)}\right)^{-1} = 0, \tag{61}$$

where we used the definition of $\mathcal{A}_{eff}$ given in Eq. (49).

The final result concerning the linear and nonlinear homogenization can be therefore summed up as follows. For the linear properties we find

$$\mathcal{L}^{(eff)} = \mathcal{L}^{(1)} + c\left(\mathcal{L}^{(2)} - \mathcal{L}^{(1)}\right)\mathcal{A}_{eff}^{-1}, \tag{62}$$

coming from Eq. (48). Similarly, for the nonlinear properties we get

$$\mathcal{N}^{(eff)} = c\left[\mathcal{I} - \left(\mathcal{L}^{(2)} - \mathcal{L}^{(1)}\right)\mathcal{A}_{eff}^{-1}(\mathcal{S} - c\mathcal{S}_d)\left(\mathcal{L}^{(1)}\right)^{-1}\right]$$
$$\times\mathcal{N}^{(2)}\mathcal{A}_{eff}^{-1}\mathcal{A}_{eff}^{-1}, \tag{63}$$

by using Eq. (57). In both results we must use the definition of $\mathcal{A}_{eff}$ given in Eq. (49), reported here for convenience

$$\mathcal{A}_{eff} = \mathcal{I} - (\mathcal{S} - c\mathcal{S}_d)\left[\mathcal{I} - \left(\mathcal{L}^{(1)}\right)^{-1}\mathcal{L}^{(2)}\right]. \tag{64}$$

It is interesting to observe that the procedure yields two results that depends only on the volume fraction c and not on the partial volume fractions Φ and Ψ. Indeed, only the value of c can be interpreted as physical volume fraction of the real composite material. We also remark that the mathematical form of the final equations is exactly the same of that obtained for the composite ellipsoid in Section 4.1. Therefore, we can say that the combination of the composite ellipsoid homogenization scheme with the (nonlinear) Mori–Tanaka theory gives, as result, the same mathematical expressions of the composite ellipsoid homogenization. It means that the Mori–Tanaka theory has the effect to generalize the procedure to the case of a dispersion of particles, without modifying the mathematical form of the equations involved. To conclude, it is important to note that Eq. (62) for the linear response, combined with Eq. (49) or (64), exactly corresponds to the Ponte Castañeda–Willis scheme (Castañeda and Willis, 1995). However, the nonlinear result stated in Eq. (63) is a new achievement with relevant theoretical and practical applications.

These results have been obtained for a second order nonlinear constitutive equation $T_{tot} = \mathcal{L}^{(2)}\varepsilon_{tot} + \mathcal{N}^{(2)}\varepsilon_{tot}\varepsilon_{tot}$. Nevertheless, they can be generalized to a constitutive equation with an arbitrary number of nonlinear terms with different orders in the strain. However, the solutions become somewhat cumbersome and are not reported here for the sake of brevity. A particular case, useful in several applications, concerns the third order relation $T_{tot} = \mathcal{L}^{(2)}\varepsilon_{tot} + \mathcal{M}^{(2)}\varepsilon_{tot}\varepsilon_{tot}\varepsilon_{tot}$, where the tensor $\mathcal{M}^{(2)}$ represents the third order response of the nonlinear particles. In this case, we eventually get the linear solution

$$\mathcal{L}^{(eff)} = \mathcal{L}^{(1)} + c\left(\mathcal{L}^{(2)} - \mathcal{L}^{(1)}\right)\mathcal{A}_{eff}^{-1}, \tag{65}$$

and the nonlinear one as

$$\mathcal{M}^{(eff)} = c\left[\mathcal{I} - \left(\mathcal{L}^{(2)} - \mathcal{L}^{(1)}\right)\mathcal{A}_{eff}^{-1}(\mathcal{S} - c\mathcal{S}_d)\left(\mathcal{L}^{(1)}\right)^{-1}\right]$$
$$\times\mathcal{M}^{(2)}\mathcal{A}_{eff}^{-1}\mathcal{A}_{eff}^{-1}\mathcal{A}_{eff}^{-1}, \tag{66}$$

where

$$\mathcal{A}_{eff} = \mathcal{I} - (\mathcal{S} - c\mathcal{S}_d)\left[\mathcal{I} - \left(\mathcal{L}^{(1)}\right)^{-1}\mathcal{L}^{(2)}\right], \tag{67}$$

similarly to Eq. (49) or (64).

We remark that when $\mathcal{L}^{(1)} = \mathcal{L}^{(2)}$ (no linear contrast between matrix and particles), we deduce from Eqs. (63) and (66) that $\mathcal{N}^{(eff)} = c\mathcal{N}^{(2)}$ and $\mathcal{M}^{(eff)} = c\mathcal{M}^{(2)}$. This means that the effective nonlinear behavior is proportional to the particles nonlinearity, with a coefficient given by the volume fraction of the dispersion. This property has been proved for composites without the ellipsoidal microstructure in earlier literature (Giordano et al., 2008, 2009; Giordano, 2009; Colombo and Giordano, 2011). Indeed, this property is manifestly true for both the cases with $\mathcal{S} = \mathcal{S}_d$ and $\mathcal{S} \neq \mathcal{S}_d$.

It is interesting to observe that our solutions, stated in Eqs. (62)–(64) for the second order nonlinearity and in Eqs. (65)–(67) for the third order nonlinearity, are also valid for an arbitrary magneto-electro-elastic (or thermo-magneto-electro-elastic) fully coupled physical behavior (Pérez-Fernández et al., 2009; Giordano et al., 2014; Giordano, 2014). In this case the tensors $\mathcal{L}^{(1)}$ and $\mathcal{L}^{(2)}$ contain all the elastic, dielectric, magnetic, piezoelectric, magnetoelastic and magnetoelectric properties and the tensors $\mathcal{N}^{(2)}$ or $\mathcal{M}^{(2)}$ describe their nonlinear counterparts. The corresponding Eshelby tensors can be calculated through well known procedures (Huang and Kuo, 1997; Huang et al., 1998). An important application concerns the combination of piezoelectric and magnetoelastic materials, which yields a stress-mediated magnetoelectric effect (Giordano et al., 2012; Koutsawa et al., 2010; Koutsawa, 2015).

7. Application to the Landau coefficients of the nonlinear elasticity

We consider here a purely elastic case and we analyse the effect of the particles distribution (ellipsoidal microstructure) on the effective nonlinear behavior of a particulate composite. The matrix is described by the linear isotropic constitutive equation $T = 2\mu_1\varepsilon + \left(K_1 - \frac{2}{3}\mu_1\right)\mathrm{Tr}(\varepsilon)\mathcal{I}$, where K_1 and μ_1 are the bulk and shear moduli, respectively. To model the inhomogeneities, we adopt the most general isotropic nonlinear constitutive equation expanded up to the second order in the strain components. It follows that the strain energy function $U(\varepsilon)$, leading to the constitutive equation $T(\varepsilon) = \frac{\partial U(\varepsilon)}{\partial\varepsilon}$, can only depend upon the principal invariants of the strain tensor, i.e. $U = U\left(\mathrm{Tr}(\varepsilon), \mathrm{Tr}(\varepsilon^2), \mathrm{Tr}(\varepsilon^3)\right)$. Therefore, by expanding $U(\varepsilon)$ up to the third order in the strain components (Giordano et al., 2008), we obtain

$$U(\varepsilon) = \mu_2\mathrm{Tr}\left(\varepsilon^2\right) + \frac{1}{2}\left(K_2 - \frac{2}{3}\mu_2\right)[\mathrm{Tr}(\varepsilon)]^2$$
$$+ \frac{A}{3}\mathrm{Tr}\left(\varepsilon^3\right) + B\mathrm{Tr}(\varepsilon)\mathrm{Tr}\left(\varepsilon^2\right) + \frac{C}{3}[\mathrm{Tr}(\varepsilon)]^3, \tag{68}$$

and deriving the stress, we get (Giordano et al., 2008)

$$T = 2\mu_2\varepsilon + \left(K_2 - \frac{2}{3}\mu_2\right)\mathrm{Tr}(\varepsilon)\hat{I}$$
$$+ A\varepsilon^2 + B\left\{\mathrm{Tr}\left(\varepsilon^2\right)\mathcal{I} + 2\varepsilon\mathrm{Tr}(\varepsilon)\right\} + C[\mathrm{Tr}(\varepsilon)]^2\mathcal{I}, \tag{69}$$

for the material corresponding to the inhomogeneites. The parameters A, B, and C are the Landau moduli (Landau and Lifschitz, 1986) and they represent the deviation from the standard linearity. It means that, in this case, we can identify the operator $\mathcal{N}^{(2)}$ through the expression $\mathcal{N}^{(2)}\varepsilon\varepsilon = A\varepsilon^2 + B\left\{\mathrm{Tr}\left(\varepsilon^2\right)\mathcal{I} + 2\varepsilon\mathrm{Tr}(\varepsilon)\right\} + C[\mathrm{Tr}(\varepsilon)]^2\mathcal{I}$. The application of the general results stated in Eqs. (62) and (63) allows us to obtain the effective nonlinear constitutive equation of the composite material as follows

$$\langle T\rangle = \left[\mathcal{L}^{(1)} + c\left(\mathcal{L}^{(2)} - \mathcal{L}^{(1)}\right)\mathcal{A}_{eff}^{-1}\right]\langle\varepsilon\rangle$$
$$+ c\left[\mathcal{I} - \left(\mathcal{L}^{(2)} - \mathcal{L}^{(1)}\right)\mathcal{A}_{eff}^{-1}(\mathcal{S} - c\mathcal{S}_d)\left(\mathcal{L}^{(1)}\right)^{-1}\right]$$
$$\times\left\{A\left(\mathcal{A}_{eff}^{-1}\langle\varepsilon\rangle\right)^2 + B\mathrm{Tr}\left[\left(\mathcal{A}_{eff}^{-1}\langle\varepsilon\rangle\right)^2\right]\mathcal{I}\right. \tag{70}$$

$$+2B\left(\mathcal{A}_{eff}^{-1}\langle\varepsilon\rangle\right)\mathrm{Tr}\left(\mathcal{A}_{eff}^{-1}\langle\varepsilon\rangle\right)$$
$$+C\left[\mathrm{Tr}\left(\mathcal{A}_{eff}^{-1}\langle\varepsilon\rangle\right)\right]^2\mathcal{I}\Big\},$$

where $\mathcal{A}_{eff}$ is given in Eq. (64).

When both regions Ω (particles) and Ω_d (ellipsoidal distribution) are spherical, we can introduce the explicit expression of the Eshelby tensor reported below (Mura, 1987)

$$\mathcal{S}_{ijkh}=\mathcal{S}_{d,ijkh}=\frac{1}{15(1-\nu_1)}\Big[\left(\delta_{ik}\delta_{jh}+\delta_{ih}\delta_{jk}\right)(4-5\nu_1)+\delta_{kh}\delta_{ij}(5\nu_1-1)\Big], \tag{71}$$

where ν_1 is the Poisson ratio of the matrix. The effect of the ellipsoidal distribution disappears and, basically, the effective constitutive equation is written as Eq. (69) where, however, the effective linear and nonlinear elastic moduli μ_{eff}, K_{eff}, A_{eff}, B_{eff}, and C_{eff} must be introduced. As for the linear elastic coefficients, we obtain

$$\mu_{eff}=\mu_1+c\frac{\mu_2-\mu_1}{c+(1-c)\left[1+\frac{6}{5}\left(\frac{\mu_2}{\mu_1}-1\right)\frac{K_1+2\mu_1}{3K_1+4\mu_1}\right]}, \tag{72}$$

$$K_{eff}=K_1+\frac{(3K_1+4\mu_1)(K_2-K_1)c}{3K_2+4\mu_1-3c(K_2-K_1)}. \tag{73}$$

Moreover, the effective Landau coefficients show a more complicated structure

$$A_{eff}=c\frac{A}{L'^2}-2c\frac{N'(\mu_2-\mu_1)}{L'^3}, \tag{74}$$

$$B_{eff}=2c\frac{\left(N'M'-L'P'\right)(\mu_2-\mu_1)}{L'^3(L'+3M')}+ -c\frac{\left(N'+3P'\right)\left[K_2-K_1-\frac{2}{3}(\mu_2-\mu_1)\right]}{L'^2(L'+3M')}+c\frac{B}{L'^2}, \tag{75}$$

$$C_{eff}=\frac{1}{9}\frac{c(9C+9B+A)}{(L'+3M')^2}+\frac{1}{9}\frac{c(A-3B)}{L'^2}+\frac{1}{9}\frac{c(4N'+6O')(\mu_2-\mu_1)}{L'^2(L'+3M')}-\frac{2}{9}\frac{c(3B+A)}{L'(L'+3M')}+\frac{1}{9}\frac{c(3N'+9P')(K_2-K_1)}{L'^2(L'+3M')}-\frac{4}{9}\frac{N'(\mu_2-\mu_1)c}{L'^3}-\frac{1}{3}\frac{c(9Q'+3O'+3P'+N')(K_2-K_1)}{(L'+3M')^3}, \tag{76}$$

where we have introduced the parameters $L'=c+(1-c)L$, $M'=(1-c)M$, $N'=(1-c)N$, $O'=(1-c)O$, $P'=(1-c)P$, and $Q'=(1-c)Q$. Finally, the parameters

$$L=1+\frac{6}{5}\frac{K_1+2\mu_1}{3K_1+4\mu_1}\left(\frac{\mu_2}{\mu_1}-1\right) \tag{77}$$

$$M=\frac{5K_2-K_1\left(3+2\frac{\mu_2}{\mu_1}\right)-4(\mu_2-\mu_1)}{5(3K_1+4\mu_1)} \tag{78}$$

$$N=\frac{3}{5}\frac{A}{\mu_1}\frac{K_1+2\mu_1}{3K_1+4\mu_1} \tag{79}$$

$$O=\frac{6}{5}\frac{B}{\mu_1}\frac{K_1+2\mu_1}{3K_1+4\mu_1} \tag{80}$$

$$P=\frac{1}{15(3K_1+4\mu_1)}\left[15B-A\left(1+3\frac{K_1}{\mu_1}\right)\right] \tag{81}$$

$$Q=\frac{1}{15(3K_1+4\mu_1)}\left[15C-2B\left(1+3\frac{K_1}{\mu_1}\right)\right] \tag{82}$$

depend on both linear and nonlinear moduli. The results stated in Eqs. (72)–(76) are in agreement with previous literature (Giordano et al., 2008, 2009; Giordano, 2009; Colombo and Giordano, 2011).

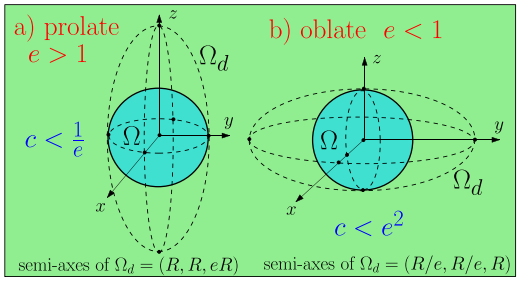

Fig. 5. Geometry of the ellipsoidal microstructure: spherical inhomogeneities of radius R surrounded by parallel security spheroids Ω_d of aspect ratio e. The smallest regions Ω_d are represented for the prolate (a) and the oblate (b) case. It is proved that the volume fraction fulfils the conditions $c<1/e$ for $e>1$ (Ω_d prolate) and $c<e^2$ for $e<1$ (Ω_d oblate).

In order to show the results for the ellipsoidal microstructure, we apply Eq. (70) to a specific geometry: we consider a dispersion of nonlinear spherical particles Ω with security surfaces Ω_d shaped as (prolate or oblate) ellipsoids of revolutions (see Fig. 5). We define the aspect ratio $e=b_z/b_x=b_z/b_y$, where (b_x, b_y, b_z) are the semi-axes of Ω_d (with $b_x=b_y$). For prolate security ellipsoids ($e>1$), the smallest Ω_d is obtained when the semi-axes are (R, R, eR), being R the radius of the spherical inhomogeneities (see Fig. 5a). In this conditions, $\Phi=1/e$ and, therefore, $c=\Phi\Psi=\Psi/e$; since $0<\Psi<1$, we have $c<1/e$ for the overall composite. Similarly, for oblate security ellipsoids ($e<1$), the smallest Ω_d is obtained when the semi-axes are $(R/e, R/e, R)$ (see Fig. 5b). In this conditions, $\Phi=e^2$ and, therefore, $c=\Phi\Psi=\Psi e^2$; since $0<\Psi<1$, we have $c<e^2$ for the overall composite. The conditions $c<1/e$ for $e>1$ and $c<e^2$ for $e<1$ can be summed up by stating that $\sqrt{c}<e<1/c$, consistently with the hypothesis of impenetrability of the security ellipsoids.

We give an example of application of Eq. (70) by considering $k_1=1000$ and $\mu_1=200$ for the matrix and $k_2=3$, $\mu_2=1.5$ and $A=B=C=10$ for the particles (in arbitrary units). Once determined the constitutive equation through Eq. (70), we can analyse the response of the overall system under deformation. When $e\neq1$, the composite material exhibits a uniaxial symmetry (transverse isotropy). Hence, we analyse both the longitudinal and transverse response.

Firstly, we apply the overall strain $\varepsilon_{ij}=0$ for $i\neq3$ and $j\neq3$ and $\varepsilon_{33}=\varepsilon$ (longitudinal deformation). We can then calculate the average stress within the composite. In particular, we consider the longitudinal component $T_{33}\triangleq T_\parallel$, which can be written as $T_\parallel=\ell_\parallel\varepsilon(1+n_\parallel\varepsilon)$, where we defined the linear and nonlinear longitudinal coefficients $\ell_\parallel$ and $n_\parallel$.

Secondly, we apply the overall strain $\varepsilon_{ij}=0$ for $i\neq1$ and $j\neq1$ and $\varepsilon_{11}=\varepsilon$ (transverse deformation). If we consider the corresponding transverse stress component $T_{11}\triangleq T_\perp$, we have $T_\perp=\ell_\perp\varepsilon(1+n_\perp\varepsilon)$, where we defined the linear and nonlinear transverse coefficients $\ell_\perp$ and $n_\perp$.

The results can be found in Fig. 6, where the linear and nonlinear, longitudinal and transverse effective coefficients are shown versus $\log_{10}e$ for different values of c. Albeit the method has been developed under the hypothesis of small c ($0<\Phi<1$ and $\Psi\ll1$), we present the results in the range $0<c<1/2$. As a matter of fact, it is not difficult to observe that the effect of the correlation (ellipsoidal symmetry) on the effective properties is of the second order in the volume fraction (Ponte Castañeda and Willis, 1995). Hence, to better understand this effect, we plotted the results in a large range of volume fraction values. For $e=1$ (green circles), we can observe the perfect correspondence between longitudinal and transverse properties since the overall material is isotropic from the elastic, both linear and nonlinear, point of view. In particular,

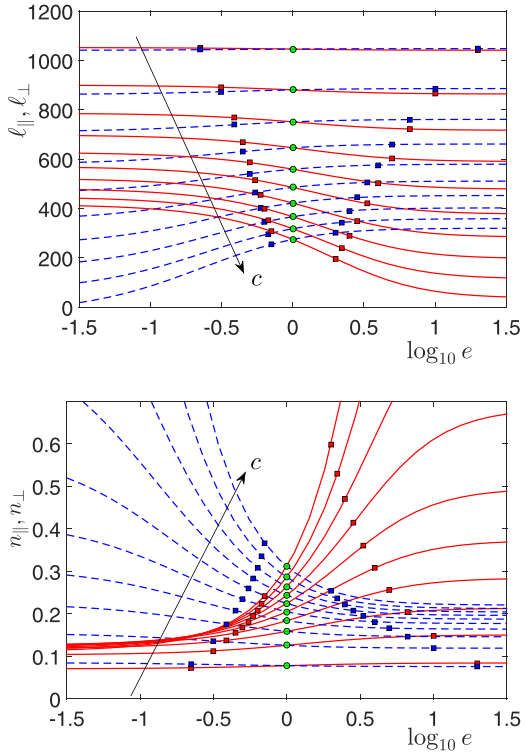

Fig. 6. Linear coefficients $\ell_\parallel$ (red continuous line) and $\ell_\perp$ (blue dashed line) and nonlinear ones $n_\parallel$ (red continuous line) and $n_\perp$ (blue dashed line) versus $\log_{10} e$ for different values of $c \in (0,\ 1/2]$ ($c = j/20\ \forall\ j = 1, \dots 20$). Square red and blue symbols represent the realistic limitations $\sqrt{c} < e < 1/c$, while the green circular symbols represent the case with $e = 1$, described by Eqs. (72)–(76). (For interpretation of the references to color in this figure legend, the reader is referred to the web version of this article.)

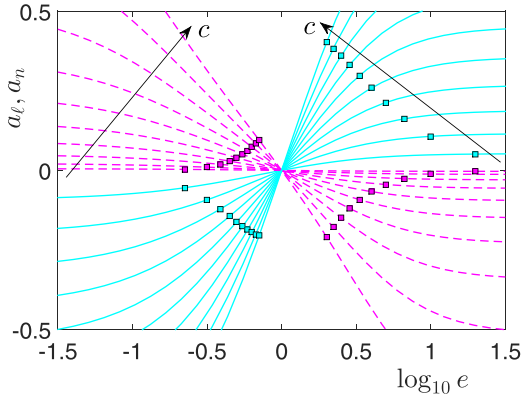

Fig. 7. Anisotropy coefficients $a_\ell = \frac{l_\perp - l_\parallel}{l_\perp + l_\parallel}$ (dashed magenta curves) and $a_n = \frac{n_\perp - n_\parallel}{n_\perp + n_\parallel}$ (solid cyan curves) versus $\log_{10} e$ and c (c assumes the same values used in Fig. 6). (For interpretation of the references to color in this figure legend, the reader is referred to the web version of this article.)

the green circular symbols are in perfect agreement with Eqs. (72)–(76), concerning the nonlinear homogenization of a dispersion of spheres without the ellipsoidal microstructure. On the other hand, for $e \neq 1$, we can observe a deviation from the classical homogenization theories, revealing the linear and nonlinear anisotropy induced by the ellipsoidal microstructure. In Fig. 6, square symbols represent the limitations $\sqrt{c} < e < 1/c$, above discussed. Interestingly enough, we observe a stronger effect of the aspect ratio e on the nonlinear response than on the linear one. Moreover, we also note a stronger effect on the nonlinear longitudinal component. This behavior is confirmed in Fig. 7 where the linear and nonlinear anisotropy coefficients $a_\ell = \frac{l_\perp - l_\parallel}{l_\perp + l_\parallel}$ and $a_n = \frac{n_\perp - n_\parallel}{n_\perp + n_\parallel}$ are represented versus e and c. These coefficients represent a normalized measure of the difference between the longitudinal and transverse responses for both the linear and nonlinear behavior. Also in Fig. 7, square symbols represent the limitation $\sqrt{c} < e < 1/c$. To conclude this analysis, we also show in Fig. 8 the total nonlinear coefficients $\ell_\perp n_\perp$ and $\ell_\parallel n_\parallel$ versus the volume fraction c for different values of the aspect ratio e. The important point is that it exists a maximum value of the nonlinear response for a given value of the volume fraction c. This result confirms previous achievements (Giordano et al., 2008, 2009; Giordano, 2009; Colombo and Giordano, 2011), represented by the thick green lines in Fig. 8 ($e = 1$), and extend their applicability to the ellipsoidal microstructure. Indeed, we can observe the effect of $e \neq 1$ (solid red and blue lines) and the bounds (dashed and dotted-dashed black lines) generated by the relation $\sqrt{c} < e < 1/c$. We can observe that the nonlinear longitudinal behavior is more influenced by the values of $e \neq 1$ than its transverse counterpart. The existence of maximum values of the nonlinear response is useful for tuning the elastic nonlinearities in composite nanomaterials (Guerder et al., 2015). The maximum point in the curve of the nonlinear features versus the volume fraction depends on the ratio k_1/k_2, defining the compressibility contrast between matrix and particles. As a matter of fact, the maximum point exists only if $k_1 \gg k_2$. Indeed, in this case, it is possible to prove that the optimal volume fraction is proportional to $k_2/k_1 \ll 1$ and the amplification of the nonlinearity is proportional to $k_1/k_2 \gg 1$. The detailed explication of the origin of the maximum value for the effective nonlinearity can be found in recent literature (Guerder et al., 2015).

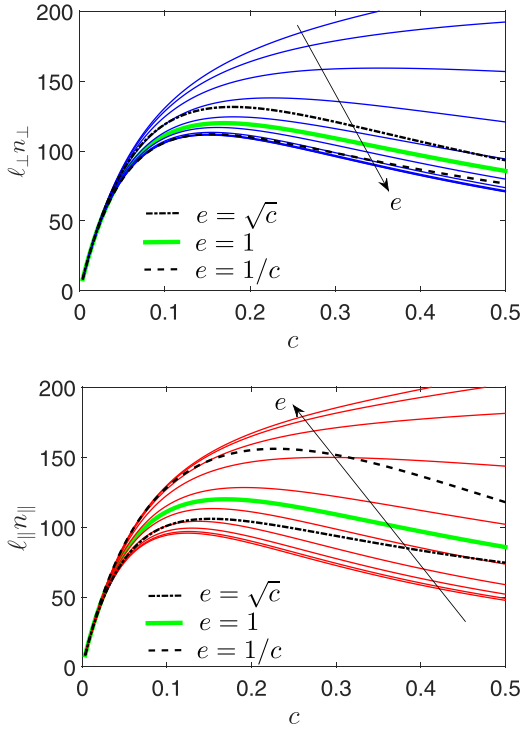

Fig. 8. Effective nonlinear coefficients $\ell_\perp n_\perp$ (solid blue lines) and $\ell_\parallel n_\parallel$ (solid red lines) versus c and e (ten values of $\log_{10} e$ in the range from -1.5 to 1.5). Thick green curves correspond to $e = 1$ and dashed and dotted-dashed black curves represent the bounds induced by the inequality $\sqrt{c} < e < 1/c$. (For interpretation of the references to color in this figure legend, the reader is referred to the web version of this article.)

8. Application to the hypersusceptibility of the nonlinear transport processes

In this Section, we consider the homogenization of the transport properties in a particulate composite material. To fix the ideas, we consider the electric conduction problem and we study the effects of the ellipsoidal microstructure on the effective conductivity of the dispersion. As it is well known, the results are equally valid for the heat conductivity, the diffusivity, the dielectric permittivity and the magnetic permeability. The matrix is characterized by a linear isotropic behavior $\mathcal{L}^{(1)} = \sigma_1 \mathcal{I}$ with a scalar conductivity σ_1 relating a current density with an electric field, i.e. $\vec{J} = \sigma_1 \vec{E}$. On the other hand, the particles are characterized by a linear conductivity σ_2 corresponding to the isotropic tensor $\mathcal{L}^{(2)} = \sigma_2 \mathcal{I}$ and by an hypersusceptibility χ describing the third order nonlinear behavior $\mathcal{M}^{(2)}\vec{E}\vec{E}\vec{E} = \chi |\vec{E}|^2 \vec{E}$. Summing up, the constitutive relation of the embedded particles can be written as $\vec{J} = \sigma_2 \vec{E} + \chi |\vec{E}|^2 \vec{E}$ (Kerr like response Giordano, 2016). Within the transport context, the Eshelby tensor of the particle (Ω) is defined as

$$\mathcal{S}_{ij} = L_i \delta_{ij}, \tag{83}$$

$$L_i = \frac{a_1 a_2 a_3}{2} \int_0^\infty \frac{d\xi}{(a_i^2 + \xi)\sqrt{\prod_{j=1}^3 (a_j^2 + \xi)}}, \tag{84}$$

where a_1, a_2 and a_3 are the semi-axes of the ellipsoid and L_i are the so-called depolarization coefficients. Similarly, the Eshelby tensor of the ellipsoid Ω_d is given by

$$\mathcal{S}_{d,ij} = L_{d,i} \delta_{ij}, \tag{85}$$

$$L_{d,i} = \frac{b_1 b_2 b_3}{2} \int_0^\infty \frac{d\xi}{(b_i^2 + \xi)\sqrt{\prod_{j=1}^3 (b_j^2 + \xi)}}, \tag{86}$$

where b_1, b_2 and b_3 are the semi-axes and $L_{d,\,i}$ are the depolarization coefficients.

We use the results obtained in Section 6, see Eqs. (65) and (66), to write the effective constitutive response of the heterogeneous material as follows

$$\begin{aligned} \langle \vec{J} \rangle = & \left[\mathcal{L}^{(1)} + c\left(\mathcal{L}^{(2)} - \mathcal{L}^{(1)}\right) \mathcal{A}_{eff}^{-1} \right] \langle \vec{E} \rangle \\ & + c\chi \left[\mathcal{I} - \left(\mathcal{L}^{(2)} - \mathcal{L}^{(1)}\right) \mathcal{A}_{eff}^{-1} (\mathcal{S} - c\mathcal{S}_d) \left(\mathcal{L}^{(1)}\right)^{-1} \right] \\ & \times \left(\mathcal{A}_{eff}^{-1} \langle \vec{E} \rangle \right) \left| \mathcal{A}_{eff}^{-1} \langle \vec{E} \rangle \right|^2, \end{aligned} \tag{87}$$

where $\mathcal{A}_{eff}$ is given in Eq. (67). This expression allows us to evaluate the effect of the particles distribution, described by the surfaces Ω_d, on both the linear and nonlinear transport properties.

For the particular case with $\mathcal{S} = \mathcal{S}_d = 1/3\mathcal{I}$, corresponding to a random distribution of spheres, we obtain the result

$$\begin{aligned} \langle \vec{J} \rangle = & \sigma_1 \frac{2\sigma_1 + \sigma_2 - 2c(\sigma_1 - \sigma_2)}{2\sigma_1 + \sigma_2 + c(\sigma_1 - \sigma_2)} \langle \vec{E} \rangle \\ & + \frac{81 c \chi \sigma_1^4}{[2\sigma_1 + \sigma_2 + c(\sigma_1 - \sigma_2)]^4} \left| \langle \vec{E} \rangle \right|^2 \langle \vec{E} \rangle, \end{aligned} \tag{88}$$

in perfect agreement with earlier findings (Yu et al., 1993; Giordano and Rocchia, 2005, 2006).

In order to show the results for the ellipsoidal microstructure, we apply Eq. (87) to the same geometry used in Section 7 (see Fig. 5). As before, for prolate security ellipsoids ($e > 1$), we have $c < 1/e$ and for oblate security ellipsoids ($e < 1$), we have $c < e^2$.

We give two examples of application of Eq. (87) by considering: (i) $\sigma_1 = 1$ for the matrix and $\sigma_2 = 10$ and $\chi = 1$ for the particles, and (ii) $\sigma_1 = 10$ for the matrix and $\sigma_2 = 1$ and $\chi = 1$ for the particles (in arbitrary units). As before, when $e \neq 1$, the composite material exhibits a transverse isotropy. Hence, we analyse both the longitudinal and transverse response.

Firstly, we apply an electric field E aligned with the z-axis and we observe the longitudinal current density $J_z = J_\parallel$, which can be written as $J_\parallel = \sigma_\parallel E(1 + \xi_\parallel E)$, where we defined the linear and nonlinear longitudinal coefficients $\sigma_\parallel$ and $\xi_\parallel$.

Secondly, we apply an electric field E aligned with the x-axis and we observe the transverse current density $J_x = J_\perp$, given by $J_\perp = \sigma_\perp E(1 + \xi_\perp E)$, where we defined the linear and nonlinear transverse coefficients $\sigma_\perp$ and $\xi_\perp$.

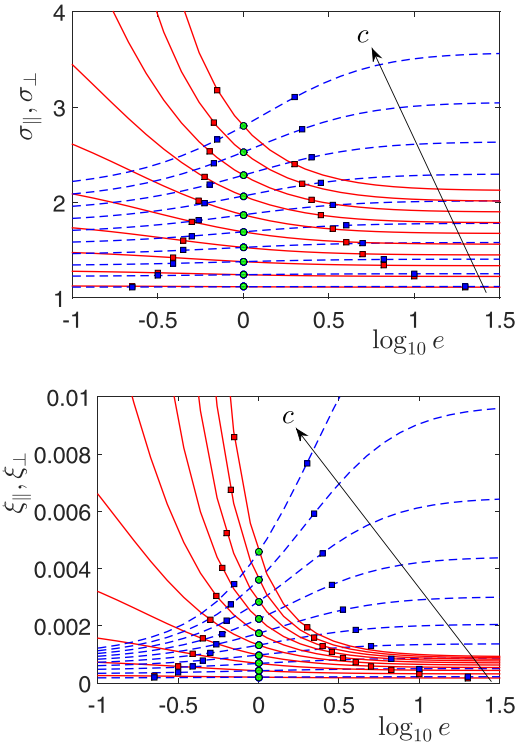

Fig. 9. Linear coefficients $\sigma_\parallel$ (red continuous line) and $\sigma_\perp$ (blue dashed line) and nonlinear coefficients $\xi_\parallel$ (red continuous line) and $\xi_\perp$ (blue dashed line). The results correspond to $\sigma_1 = 1$, $\sigma_2 = 10$ and $\chi = 1$ and are plotted versus $\log_{10} e$ for different values of $c \in (0, 1/2]$ ($c = j/20\ \forall\ j = 1, \ldots 20$). Square red and blue symbols represent the realistic limitations $\sqrt{c} < e < 1/c$, while the green circular symbols represent the case with $e = 1$, described by Eq. (88). (For interpretation of the references to color in this figure legend, the reader is referred to the web version of this article.)

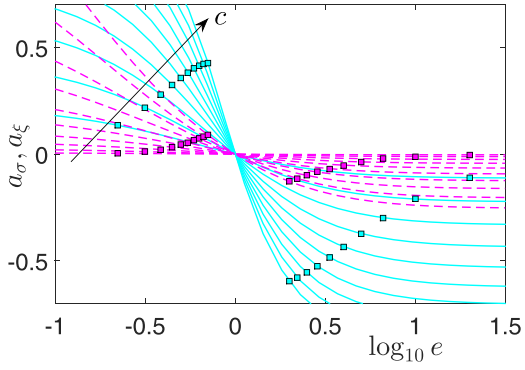

Fig. 10. Anisotropy coefficients $a_\sigma = \frac{\sigma_\perp - \sigma_\parallel}{\sigma_\perp + \sigma_\parallel}$ (dashed magenta curves) and $a_\xi = \frac{\xi_\perp - \xi_\parallel}{\xi_\perp + \xi_\parallel}$ (solid cyan curves) versus $\log_{10} e$ and c (c assumes the same values used in Fig. 9). The results correspond to $\sigma_1 = 1$, $\sigma_2 = 10$ and $\chi = 1$. (For interpretation of the references to color in this figure legend, the reader is referred to the web version of this article.)

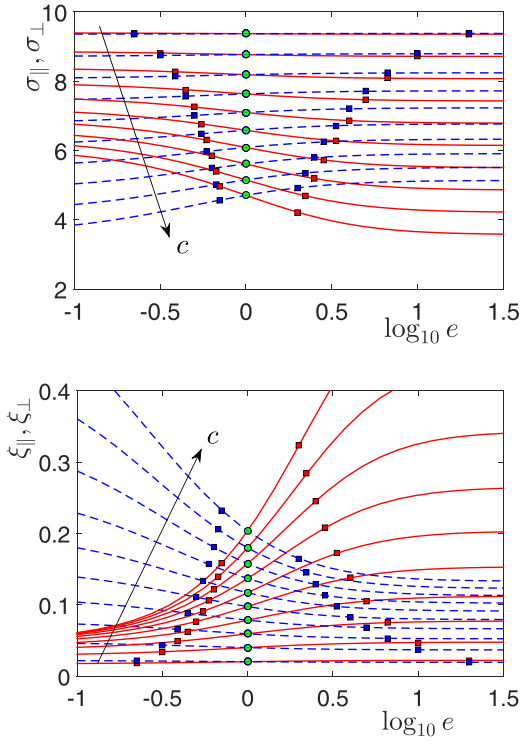

Fig. 11. Linear coefficients $\sigma_\parallel$ (red continuous line) and $\sigma_\perp$ (blue dashed line) and nonlinear coefficients $\xi_\parallel$ (red continuous line) and $\xi_\perp$ (blue dashed line). The results correspond to $\sigma_1 = 10$, $\sigma_2 = 1$ and $\chi = 1$ and are plotted versus $\log_{10} e$ for different values of $c \in (0, 1/2]$ ($c = j/20 \; \forall \; j = 1, \ldots 20$). Square red and blue symbols represent the realistic limitations $\sqrt{c} < e < 1/c$, while the green circular symbols represent the case with $e = 1$, described by Eq. (88). (For interpretation of the references to color in this figure legend, the reader is referred to the web version of this article.)

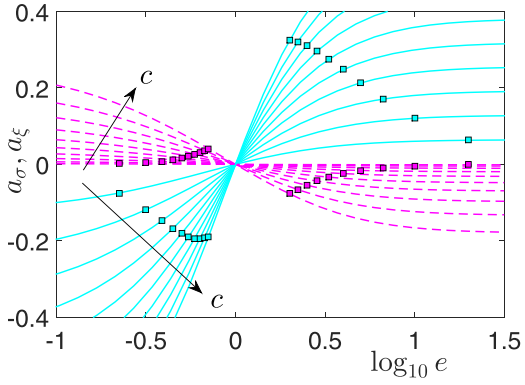

Fig. 12. Anisotropy coefficients $a_\sigma = \frac{\sigma_\perp - \sigma_\parallel}{\sigma_\perp + \sigma_\parallel}$ (dashed magenta curves) and $a_\xi = \frac{\xi_\perp - \xi_\parallel}{\xi_\perp + \xi_\parallel}$ (solid cyan curves) versus $\log_{10} e$ and c (c assumes the same values used in Fig. 11). The results correspond to $\sigma_1 = 10$, $\sigma_2 = 1$ and $\chi = 1$. (For interpretation of the references to color in this figure legend, the reader is referred to the web version of this article.)

The results are shown in Figs. 9 and 10 for the first set of parameters ($\sigma_1 = 1$, $\sigma_2 = 10$ and $\chi = 1$) and in Figs. 11 and 12 for the second set ($\sigma_1 = 10$, $\sigma_2 = 1$ and $\chi = 1$). For both sets of parameters, we can observe the coincidence of longitudinal and transverse results for $e = 1$ (see, e.g., green circles in Figs. 9 and 11): this is in agreement with earlier theories represented by Eq. (88). Moreover, we note a deviation from this result when $e \neq 1$. In this case, we can notice a stronger influence of the aspect ratio e on the nonlinear properties than on the linear ones. Besides, the longitudinal nonlinear response is even more affected by e than its transverse counterpart. By comparing the two set of parameters adopted, we can deduce that the effective nonlinear response of the system is larger if $\sigma_1 > \sigma_2$. In addition, we note that, when $\sigma_1 > \sigma_2$, $\xi_\parallel$ is an increasing function of e while $\xi_\perp$ is a decreasing function of e. On the other hand, when $\sigma_2 > \sigma_1$, $\xi_\parallel$ is a decreasing function of e while $\xi_\perp$ is an increasing function of e. This behavior can be also deduced from Figs. 10 and 12 where the anisotropy coefficients $a_\sigma = \frac{\sigma_\perp - \sigma_\parallel}{\sigma_\perp + \sigma_\parallel}$ (dashed magenta curves) and $a_\xi = \frac{\xi_\perp - \xi_\parallel}{\xi_\perp + \xi_\parallel}$ (solid cyan curves) are shown versus $\log_{10} e$ and c. Indeed, while the sign of a_σ (see dashed magenta curves) is the same for the two sets of parameters (for the same value of e), the sign of a_ξ (see solid cyan curves) is different for the cases $\sigma_1 > \sigma_2$ and $\sigma_2 > \sigma_1$. This complex scenario proves the importance of considering the real distribution of inhomogeneities (e.g., the elliposidal microstructure) when studying the nonlinear properties of dispersions of particles. In particular, this is relevant for the synthesis or the analysis of nanocomposites with tuned nonlinear effective response.

9. Conclusions

A nonlinear homogenization scheme is presented for analysing dispersions of particles exhibiting an ellipsoidal microstructure. It means that we can evaluate the effects of the real distribution of particles on the linear and nonlinear effective behavior of the heterogeneous material. Under this respect, we can say that we have generalized the classical Ponte Castañeda–Willis theory in order to take into account the nonlinear features of the composite. We adopted a two-step multiscale approach taking account the constitutive nonlinearity at the underling level and the statistical distribution at the intermediate level. The first step is based on the definition of an ellipsoidal security surface describing the correlation of the particle positions. Moreover, the second step represents a nonlinear generalization of the Mori–Tanaka scheme. While this methodology is able to consider both the correlation and the nonlinearity of the particles, the non-local effects emerging by the microstrucure have been neglected in this context. Through two examples, dealing with elastic and transport properties, we showed that the nonlinear effective response can be significantly modified by the actual distribution of particles, in particular when described by the ellipsoidal microstructure. Indeed, we observed the linear and nonlinear anisotropic behavior induced by the ellipsoidal correlation among the inhomogeneities. These effects play an important role for studying the nonlinear composite structures used in diverse technological applications, including acoustic, electromagnetic and multiphysics devices. Moreover, the proposed approach can be used for validating advanced numerical models and multiscale techniques, largely used for the description of materials with random microstructure.

References

Bacca, M., Bigoni, D., Corso, F.D., Veber, D., 2013a. Mindlin second-gradient elastic properties from dilute two-phase cauchy-elastic composites. Part I: closed form expression for the effective higher-order constitutive tensor. Int. J. Sol. Struct. 50, 4010–4019.

Bacca, M., Bigoni, D., Corso, F.D., Veber, D., 2013b. Mindlin second-gradient elastic properties from dilute two-phase cauchy-elastic composites. Part II: higher-order constitutive properties and application cases. Int. J. Sol. Struct. 50, 4020–4029.

Berger, V., 1998. Nonlinear photonic crystals. Phys. Rev. Lett. 81, 4136.

Berryman, J.G., 1997. Generalization of eshelbys formula for a single ellipsoidal elastic inclusion to poroelasticity and thermoelasticity. Phys. Rev. Lett. 79, 1142.

Brunet, T., Leng, J., Mondain-Monval, O., 2013. Soft acoustic metamaterials. Science 342, 323.

Cauvin, L., Kondo, D., Brieu, M., Bhatnagar, N., 2010. Mechanical behavior of a PP platelet-reinforced nanocomposite: experimental characterization and two scale modeling of linear and non-linear response. Mater. Sci. Eng. A 527, 1102–1108.

Colombo, L., Giordano, S., 2011. Nonlinear elasticity in nanostructured materials. Rep. Prog. Phys. 74, 116501.

Dormieux, L., Kondo, D., 2016. Micromechanics of Fracture and Damage. ISTE Ltd., John Wiley & Sons, Inc., London.

Dormieux, L., Molinari, A., Kondo, D., 2002. Micromechanical approach to the behavior of poroelastic materials. J. Mech. Phys. Solids 50, 2203.

Eshelby, J.D., 1957. The determination of the elastic field of an ellipsoidal inclusion and related problems. Proc. R. Soc. Lond. A 241, 376.
Eshelby, J.D., 1959. The elastic field outside an ellipsoidal inclusion. Proc. R. Soc. Lond. A 252, 561.
Franciosi, P., 2013. Transversally isotropic magneto-electro-elastic composites with co-(dis) continuous phases. Int. J. Solids Struct. 50, 1013.
Galipeau, E., Ponte Castañeda, P., 2012. The effect of particle shape and distribution on the macroscopic behavior of magnetoelastic composites. Int. J. Solids Struct. 49, 1.
Ghosh, S., 2011. Micromechanical Analysis and Multi-scale Modeling Using the Voronoi Cell Finite Element Method. CRC Press, Taylor and Francis, Boca Raton.
Giordano, S., 2003. Differential schemes for the elastic characterization of dispersions of randomly oriented ellipsoids. Eur. J. Mech. A/Solids. 22, 885–902.
Giordano, S., 2005. Order and disorder in heterogeneous material microstructure: electric and elastic characterization of dispersions of pseudo-oriented spheroids. Int. J. Eng. Sci. 43, 1033.
Giordano, S., 2009. Dielectric and elastic characterization of nonlinear heterogeneous materials. Materials 2, 1417.
Giordano, S., 2013. Analytical procedure for determining the linear and nonlinear effective properties of the elastic composite cylinder. Int. J. Solids Struct. 50, 4055–4069.
Giordano, S., 2014. Explicit nonlinear homogenization for magneto-electro-elastic laminated materials. Mech. Res. Comm. 55, 18–29.
Giordano, S., 2016. Nonlinear effective behavior of a dispersion of randomly oriented coated ellipsoids with arbitrary temporal dispersion. Int. J. Eng. Sci. 98, 14.
Giordano, S., Colombo, L., 2007a. Effects of the orientational distribution of cracks in isotropic solids. Eng. Fract. Mech. 74, 1983.
Giordano, S., Colombo, L., 2007b. Effects of the orientational distribution of cracks in solids. Phys. Rev. Lett. 98, 055503.
Giordano, S., Dusch, Y., Tiercelin, N., Pernod, P., Preobrazhensky, V., 2012. Combined nanomechanical and nanomagnetic analysis of magnetoelectric memories. Phys. Rev. B 85, 155321.
Giordano, S., Goueygou, M., Tiercelin, N., Talbi, A., Pernod, P., Preobrazhensky, V., 2014. Magneto-electro-elastic effective properties of multilayered artificial multiferroics with arbitrary lamination direction. Int. J. Eng. Sci. 78, 134–153.
Giordano, S., Palla, P.L., Colombo, L., 2008. Nonlinear elastic Landau coefficients in heterogeneous materials. Euro Phys. Lett. 83, 66003.
Giordano, S., Palla, P.L., Colombo, L., 2009. Nonlinear elasticity of composite materials. Eur. Phys. J. B 68, 89.
Giordano, S., Rocchia, W., 2005. Shape-dependent effects of dielectrically nonlinear inclusions in heterogeneous media. J. Appl. Phys. 98, 104101.
Giordano, S., Rocchia, W., 2006. Predicting the dielectric nonlinearity of anisotropic composite materials via tensorial analysis. J. Phys. Condens. Matter 18, 10585.
Gruescu, C., Giraud, A., Homand, F., Kondo, D., Do, D.P., 2007. Effective thermal conductivity of partially saturated porous rocks. Int. J. Solids Struct. 44, 811.
Guerder, P.-Y., Giordano, S., Matar, O.B., Vasseur, J.O., 2015. Tuning the elastic nonlinearities in composite nanomaterials. J. Phys.: Condens. Matter 27, 145304.
Herbold, E.B., Nesterenko, V.F., 2013. Propagation of rarefaction pulses in discrete materials with strain-softening behavior. Phys. Rev. Lett. 110, 144101.
Hu, G.K., Weng, G.J., 2000a. The connections between the double inclusion model and the Ponte Castañeda–Willis, mori-tanaka, and Kuster–Toksoz models. Mech. Mater. 32, 495–503.
Hu, G.K., Weng, G.J., 2000b. Some reflections on the mori-tanaka and Ponte Castañeda–Willis methods with randomly oriented ellipsoidal inclusions. Acta Mech. 140, 31–40.
Huang, J.H., Chiu, Y.H., Liu, H.K., 1998. Magneto-electro-elastic eshelby tensors for a piezoelectric-piezomagnetic composite reinforced by ellipsoidal inclusions. J. Appl. Phys. 83, 5364.
Huang, J.H., Kuo, W.S., 1997. The analysis of piezoelectric/piezomagnetic composite materials containing ellipsoidal inclusions. J. Appl. Phys. 81, 1378.
Kachanov, M., 1994. Elastic solids with many cracks and related problems. Adv. Appl. Mech. 30, 259–445.
Kachanov, M., Sevostianov, I., 2005. On quantitative characterization of microstructures and effective properties. Int. J. Solids Struct. 42, 309–336.
Kanaun, S., Levin, V., 2008. Self-consistent methods for composites. Static Problems, 1. Springer, Dordrecht.
Kanaun, S., Levin, V., 2008. Self-consistent methods for composites. Wave Propagation in Heterogeneous Materials, 2. Springer, Dordrecht.
Kim, E., Kim, Y.H.N., Yang, J., 2015. Nonlinear stress wave propagation in 3d woodpile elastic metamaterials. Int. J. Solids Struct. 58, 128–135.
Koutsawa, Y., 2015. Overall thermo-magneto-electro-elastic properties of multiferroics composite materials with arbitrary heterogeneities spatial distributions. Compos. Struct. 133, 764.
Koutsawa, Y., Biscani, F., Belouettar, S., Nasser, H., Carrera, E., 2010. Multi-coating inhomogeneities approach for the effective thermo-electro-elastic properties of piezoelectric composite materials. Compos. Struct. 92, 964.
Kozyrev, A.B., van der, W., 2008. Nonlinear left-handed transmission line metamaterials. J. Phys. D: Appl. Phys. 41, 173001.
Kröner, E., 1990. Modified green functions in the theory of heterogeneous and/or anisotropic linearly elastic media. In: Weng, G.J., et al. (Eds.), Micromechanics and Inhomogeneity. Springer-Verlag, New York Inc.
Landau, L.D., Lifschitz, E.M., 1986. Theory of Elasticity. Butterworth Heinemann, Oxford.
Lapine, M., Shadrivov, I.V., Kivshar, Y.S., 2014. Colloquium: nonlinear metamaterials. Rev. Mod. Phys. 86, 1093.
Lapine, M., Shadrivov, I.V., Powell, D.A., Kivshar, Y.S., 2012. Magnetoelastic metamaterials. Nat. Mater. 11, 30–33.
Li, N., Ren, J., Wang, L., Zhang, G., Hänggi, P., Li, B., 2012. Phononics: manipulating heat flow with electronic analogs and beyond. Rev. Mod. Phys. 84, 1045.
Li, S., Wang, G., 2008. Introduction to Micromechanics and Nanomechanics. World Scientific, Singapore.
Liang, B., Guo, X.S., Tu, J., Zhang, D., Cheng, J.C., 2010. An acoustic rectifier. Nat. Mater. 9, 989.
Liang, B., Yuan, B., Cheng, J.C., 2009. Acoustic diode: rectification of acoustic energy flux in one-dimensional systems. Phys. Rev. Lett. 103, 104301.
Lydon, J., Theocharis, G., Daraio, C., 2015. Nonlinear resonances and energy transfer in finite granular chains. Phys. Rev. E 91, 023208.
Manktelow, K., Leamy, M.J., Ruzzene, M., 2011. Multiple scales analysis of wave-wave interactions in a cubically nonlinear monoatomic chain. Nonlinear Dyn. 63, 193–203.
Mary, A., Rodrigo, S.G., Martín-Moreno, L., García-Vidal, F.J., 2008. Plasmonic metamaterials based on holey metallic films. J. Phys.: Condens. Matter 20, 304215.
Milton, G.W., 2002. The Theory of Composites. Cambridge University Press, Cambridge.
Mingaleev, S., Kivshar, Y., 2002. Nonlinear photonic crystals: toward all-optical technologies. Opt. Photonics News 13, 48–51.
Mori, T., Tanaka, K., 1973. Average stress in matrix and average elastic energy of materials with misfitting inclusions. Acta Metall. 21, 571–574.
Mura, T., 1987. Micromechanics of Defects in Solids. Kluwer Academic Publishers, Dordrecht.
Nemat-Nasser, S., Hori, M., 1993. Micromechanics: Overall Properties of Heterogeneous Materials. North-Holland, Amsterdam.
Ostoja-Starzewski, M., 2006. Material spatial randomness: from statistical to representative volume element. Probabilist Eng. Mech. 21, 112–132.
Palla, P.L., Giordano, S., Colombo, L., 2010. Lattice model describing scale effects in nonlinear elasticity of nanoinhomogeneities. Phys. Rev. B 81, 214113.
Pérez-Fernández, L.D., Bravo-Castillero, J., Rodríguez-Ramos, R., Sabina, F.J., 2009. On the constitutive relations and energy potentials of linear thermo-magnetoelectro-elasticity. Mech. Res. Commun. 36, 343.
Ponte Castañeda, P., 1991. The effective mechanical properties of nonlinear isotropic composites. J. Mech. Phys. Solids 39, 45–71.
Ponte Castañeda, P., 1992. Bounds and estimates for the properties of nonlinear heterogeneous systems. Philos. Trans. R. Soc. Lond. A 340, 531–567.
Ponte Castañeda, P., Willis, J.R., 1995. The effect of spatial distribution on the effective behavior of composite materials and cracked media. J. Mech. Phys. Solids 43, 1919.
Ponte Castañeda, P., Suquet, P., 1998. Nonlinear composites. Adv. Appl. Mech. 34, 171–302.
Porter, M., Kevrekidis, P., Daraio, C., 2015. Granular crystals: nonlinear dynamics meets materials engineering. Phys. Today 68, 44.
Qu, J., Cherkaoui, M., 2006. Fundamentals of Micromechanics of Solids. John Wiley & Sons, Inc., Hoboken, New Jersey.
Rose, A., Huang, D., Smith, D.R., 2012. Demonstration of nonlinear magnetoelectric coupling in metamaterials. Appl. Phys. Lett. 101, 051103.
Salmi, M., Auslender, F., Bornert, M., Fogli, M., 2012. Apparent and effective mechanical properties of linear matrix-inclusion random composites: improved bounds for the effective behavior. Int. J. Solids Struct. 49, 1195–1211.
Soljacic, M., Joannopoulos, J.D., 2010. Enhancement of nonlinear effects using photonic crystals. Nat. Mater. 3, 211.
Suquet, P., 1993. Overall potentials and extremal surfaces of power law or ideally plastic composites. J. Mech. Phys. Solids 41, 981–1002.
Talbot, D.R.S., Willis, J.R., 1985. Variational principles for inhomogeneous nonlinear media. J. Appl. Math. 35, 39.
Talbot, D.R.S., Willis, J.R., 1987. Bounds and self-consistent estimates for the overall properties of nonlinear composites. J. Appl. Math. 39, 215–240.
Tanaka, K., Mori, T., 1972. Note on volume integrals of the elastic field around an ellipsoidal inclusion. J. Elast. 2, 199.
Torquato, S., 2002. Random Heterogeneous Materials. Springer-Verlag, New York.
Trovalusci, P., De Bellis, M.L., Ostoja-Starzewski, M., Murrali, A., 2014. Particulate random composites homogenized as micropolar materials. Meccanica 49, 2719–2727.
Trovalusci, P., Ostoja-Starzewski, M., De Bellis, M.L., Murrali, A., 2015. Scale-dependent homogenization of random composites as micropolar continua. Eur. J. Mech. A/Solids 49, 396–407.
Tsang, H.K., Liu, Y., 2008. Nonlinear optical properties of silicon waveguides. Semicond. Sci. Technol. 23, 064007.
Wendt, A.S., Bayuk, I.O., Covey-Crump, S.J., Wirth, R., Lloyd, G.E., 2003. An experimental and numerical study of the microstructural parameters contributing to the seismic anisotropy of rocks. J. Geophys. Res. 108 (B8), 2365.
Weng, G.J., 2010. A dynamical theory for the Mori–Tanaka and Ponte Castañeda–Willis estimates. Mech. Mater. 42, 886–893.
Willis, J.R., 1977. Bounds and self-consistent estimates for the overall properties of anisotropic composites. J. Mech. Phys. Solids 25, 185.
Willis, J.R., 1978. Variational principles and bounds for the overall properties of composites. In: Provan, J.W. (Ed.), Continuum Models for Discrete Systems. University of Waterloo Press, Waterloo, pp. 185–215.
Xu, G., Pan, T., Zang, T., Sun, J., 2009. Nonlinear surface polaritons in anisotropic kerr-type metamaterials. J. Phys. D: Appl. Phys. 42, 045303.
Yu, K.W., Hui, P.M., Stroud, D., 1993. Effective dielectric response of nonlinear composites. Phys. Rev. B 47, 14150.